

Supporting Information

for

Optimizing the Chloroallene Pathway Toward the One-Pot Synthesis of Rubrene

Alberto Ongaro,^a Matteo Benetazzo,^a Giulia Tecchio,^a Simone Silvestrini,^{a†} Federico Rastrelli,^a Luca Vaghi,^b Antonio Papagni,^b Tommaso Carofiglio,^a Michele Maggini^{a,c}

^a Department of Chemical Sciences, University of Padova, Via F. Marzolo 1, 35131 Padova, Italy.

^b Department of Materials Science, University of Milano Bicocca, Via R. Cozzi 53, 20125 Milano, Italy.

^c Institute of Condensed Matter Chemistry and Technologies for Energy ICMATE-CNR, Corso Stati Uniti 4, 35127 Padova, Italy

[†] S.S. present address: Procter and Gamble, Brussels Innovation Centre, Temselaan 100, Strombeek-bever, B-1853, Belgium.

TABLE OF CONTENTS

1. Materials and Methods

2. Identification of the most effective chloride-based reagent for converting TPPA into TPCA

2.1 Optimization of the ¹³C NMR assay for the detection of TPCA

2.2 ¹³C NMR UDEFT method for the characterization of reaction crudes

2.3 HPLC-MS method for the characterization of reaction crudes

2.4 Reaction of TPPA with different chloride-based reagents

2.4.1 Oxalyl chloride

2.4.2 Methanesulfonyl chloride

2.4.3 Phosphorus pentachloride

2.4.4 Vilsmeier reagent

2.4.5 Triphenyl phosphine dichloride

3. Optimization of the one-pot synthesis of rubrene

3.1. Determination of rubrene concentration by UV-Vis spectroscopy

3.2. Synthesis of rubrene with PCl₅: reaction conditions screening

3.3. Synthesis of rubrene with TMSCl

3.4. NMR yield quantification of rubrene (PCl₅, conventional heating - M1)

3.5. NMR yield quantification of rubrene (PCl₅, microwave heating - M2)

3.6. NMR of rubrene (exp. 6, Table S4)

3.7. ¹H NMR of rubrene from the scale-up experiment (TMSCl, conventional heating - M3)

3.8. NMR and UPLC-HRMS analysis of TPE (exp. 6, Table S4)

4. NMR characterization of cyclobutene 6 and rubrene endoperoxide

5. ¹³C NMR UDEFT spectra

1. Materials and Methods

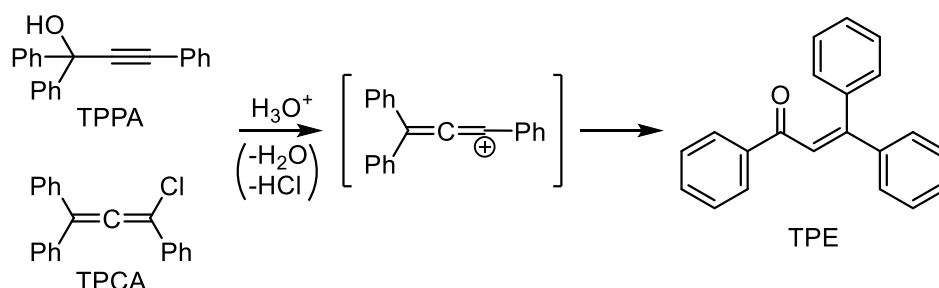
Chemicals were purchased from Merck and used without further purification. 3-Methyl-1,2-butadiene and rubrene are commercially available reagents. Solvents were analytical grade products. NMR spectra were recorded on a Bruker 500 Avance III operating at 500 MHz (¹H: 500 MHz, ¹³C: 125 MHz) or on a Bruker AF-300 operating at 300 MHz (¹H: 300 MHz, ¹³C: 75 MHz). The spectra were elaborated with MestreNova software. Chemical shifts are given in ppm at room temperature and are referenced to residual protic impurities in the solvent. The resonance multiplicities are indicated as “s” (singlet), “d” (doublet), “m” (multiplet). UV-Vis spectra were recorded on a Varian Cary 50 UV-

Vis spectrophotometer using quartz cuvettes with a 1 cm path length. HPLC conditions and instrumentation are described in Section 2.3. UPLC–HRMS analyses were performed on an ACQUITY UPLC I-Class PLUS system equipped with an ACQUITY PDA eλ Detector set at 254 nm and a high-resolution time-of-flight (ToF) mass analyzer with an electrospray ionization (ESI) source (ACQUITY RDa Detector; Waters Corporation). Chromatographic separation was achieved using a Kinetex® EVO C18 column (2.6 μm, 100 Å, 100 × 2.1 mm; Phenomenex). The mobile phases consisted of water containing 0.1% formic acid (A) and acetonitrile containing 0.1% formic acid (B). The gradient elution was from 5% to 100% B over 15 min, followed by 3 min at 100% B. The injection volume was 1 μl.

Identification of the most effective chloride-based reagent for converting TPPA into TPCA

2.1. Optimization of the ¹³C NMR assay for the detection of TPCA

We investigated the formation of the key intermediate TPCA **2** from TPPA **5**, with the goal of identifying the most effective chloride-based reagent and clarifying the side reactions that limit yields. However, when we tried to purify TPCA from the crude mixtures by silica-gel column chromatography, it developed an intense red color that vanished in about 30 s giving a yellowish eluate. An analogous behaviour was observed during TLC analyses as soon as the spot of crude mixture was deposited on the silica gel layer. Column chromatography afforded only TPE, whereas TPCA was most likely degraded during elution. We reasonably assume that the acidity of SiO₂, together with traces of water, promoted its conversion into TPE via a Meyer–Schuster rearrangement, as illustrated in Scheme S1.



Scheme S1. Formation of TPE.

These observations made the isolation and quantification of TPCA by standard purification techniques challenging. We therefore reasoned that a non-destructive method such as ¹³C NMR spectroscopy would allow us to estimate the relative amounts of TPCA and TPE directly in the crude mixture. Notably, in the context of rubrene synthesis, TPE constitutes an additional drawback because its formation consumes TPCA and/or TPPA. Conveniently, the allene carbon of TPCA and the carbonyl carbon of TPE resonate in otherwise uncrowded regions of the ¹³C NMR spectrum, at 203.8 and 192.3 ppm, respectively, as shown in Figure S1.

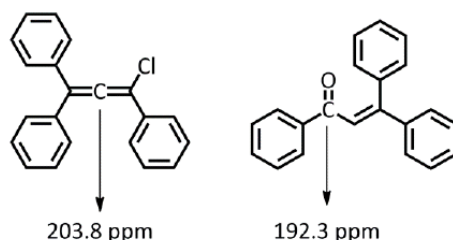


Figure S1. Allene and carbonyl carbon chemical shift.

The main drawback of ¹³C NMR characterization is the long relaxation times associated to both allene and carbonyl carbons of TPCA and TPE (> 1 min). Under these conditions, the time needed to record a ¹³C NMR spectrum with a reliable S/N ratio may be enough for TPCA to convert into TPE. Figure S2 shows the ¹³C NMR spectrum of a representative crude mixture obtained by reacting TPPA with PCl₅ at 0 °C in the presence of DBU for 90 min in CH₂Cl₂ (using a TPPA/PCl₅/DBU ratio of 1:1.3:2.5 at a TPPA concentration of 0.14 M) then 500 μl of the crude mixture were mixed with 200

μl of CD_2Cl_2 and directly analysed. Figure S3 reports the ^{13}C NMR spectrum of the same sample after a 48 h acquisition, where the disappearance of the signal at 204 ppm is clearly evident.

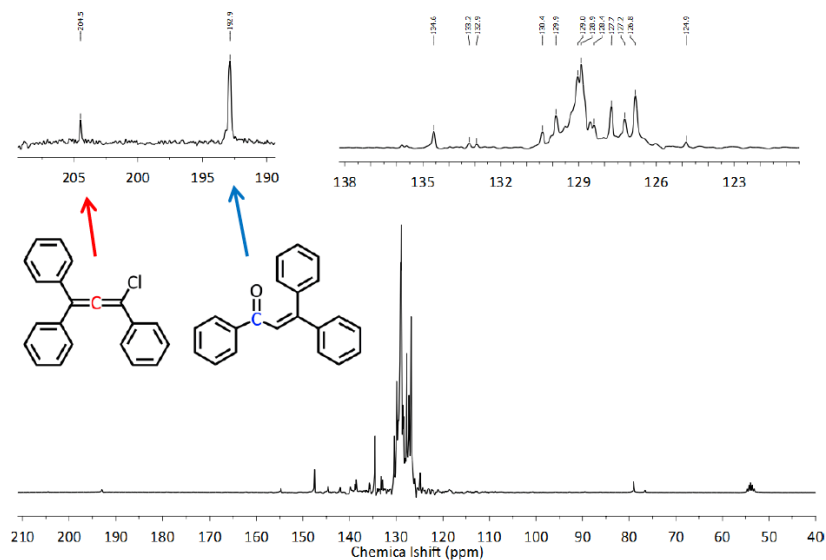


Figure S2. ^{13}C NMR (CD_2Cl_2 , 75 MHz) spectrum of a crude mixture (see text) containing TPCA and TPE (relaxation time < 1 min).

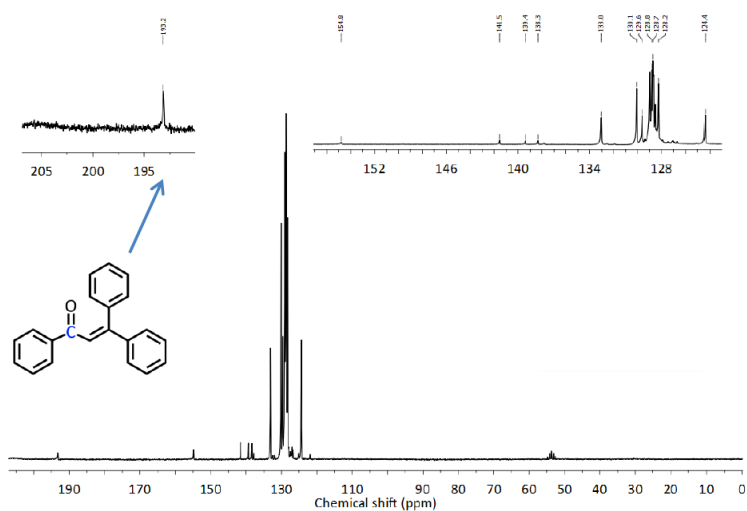


Figure S3. ^{13}C NMR (CD_2Cl_2 , 75 MHz) spectrum of the same mixture as in Figure S2, recorded after 48 h (relaxation time < 1 min).

Furthermore, allene and carbonyl carbons need long relaxation times (T_1) and relaxation delay (RD) to avoid saturation. Figure S4 shows a ^{13}C NMR spectrum of the mixture TPCA and TPE after 48 h acquisition time using a zlg30 sequence that avoids saturation of the two quaternary carbons. The spectrum is nice but the relative ratio of TPCA and TPE is affected by the reactivity of TPCA as discussed above.

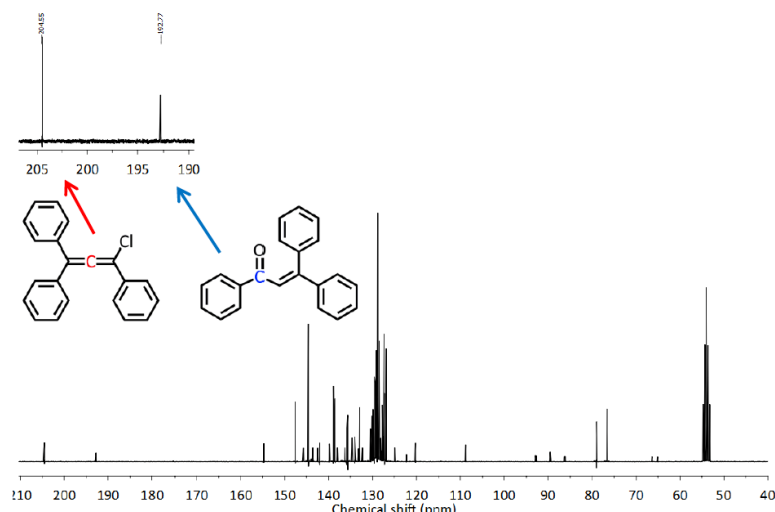


Figure S4. TPCA and TPE not saturated ^{13}C NMR (CD_2Cl_2 , 75 MHz) spectrum.

To overcome the problems of reactivity and signal saturation, ^{13}C NMR UDEFT spectroscopy was employed in its implementation without heteronuclear NOE [M. Piotta, M. B., K. Elbayed, J. Wieruszski, G. Lippens, *Magnetic Resonance in Chemistry* **2006**, 44]. The optimization of this methodology is presented below, whereas the technique itself will be employed to gather useful data on the reaction of TPPA with chloride-based reagents. ^{13}C NMR UDEFT experiments were first carried out on two standards: pure TPE, that was synthesized as reported in the literature, and commercial 3-methyl-1,2-butadiene (3MBD, Figure S5) in place of reactive intermediate TPCA, assuming a similar NMR behaviour of the allene carbon for both compounds.

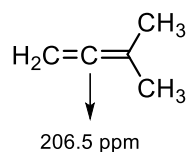


Figure S5. 3-methyl-1,2-butadiene (3MBD).

A stock solution was prepared by dissolving, in 1 ml of CH_2Cl_2 , TPE (22.1 mg, 0.07 mmol, 77 mM) and 3MBD (10.2 mg, 0.15 mmol, 149 mM). The NMR tube was prepared introducing 200 μl of the stock solutions, 100 μl of CH_2Cl_2 and 200 μl of CD_2Cl_2 . The final concentration of TPE and 3MBD was 22 and 43 mM, respectively (Figure S6 and S7).

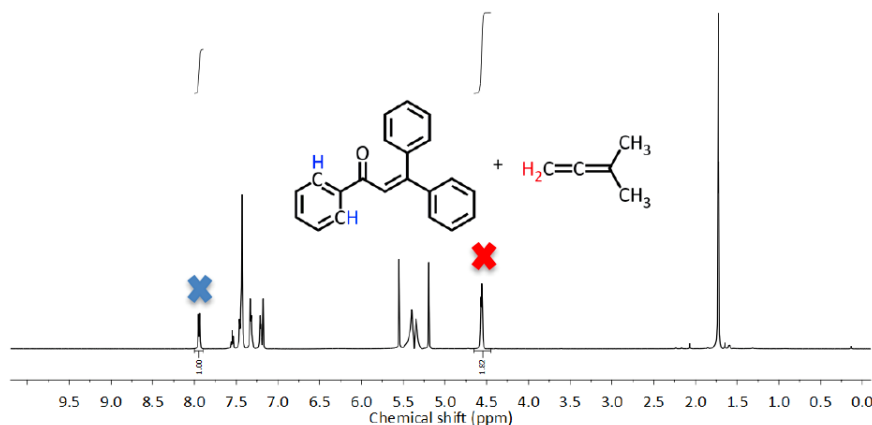


Figure S6. ^1H NMR (CD_2Cl_2 , 500 MHz) spectrum of TPE and 3MBD (22 and 43 mM respectively).

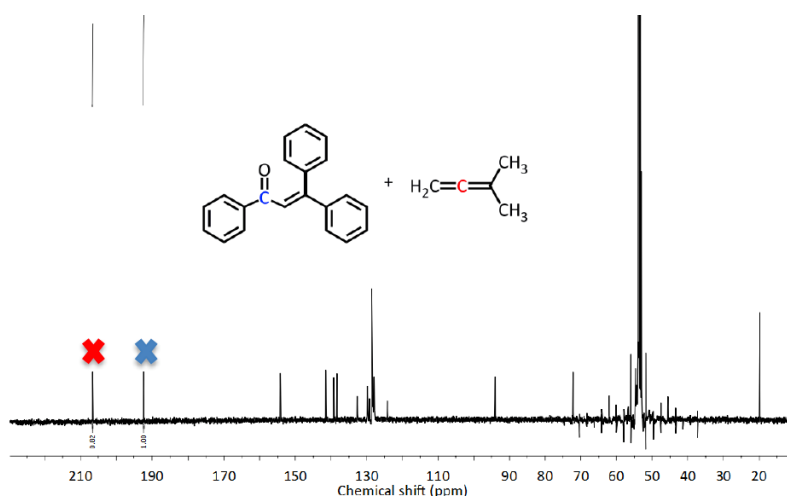


Figure S7. ^{13}C NMR UDEFT spectrum (CD_2Cl_2 , 125 MHz) of TPE and 3MBD (22 and 43 mM respectively).

The calculated TPE/3MBD ratio by ^1H NMR and ^{13}C NMR is 1.00/1.81 and 1.00/0.95 respectively, with an apparent signal loss for the allene carbon of about 50%. As a matter of fact, TPE was never detected in the NMR samples that were analysed with the UDEFT sequence. Nonetheless, the UDEFT experiment remains a versatile tool that allows the rapid acquisition of ^{13}C NMR spectra of molecules such as TPCA, that suffer from degradation during long acquisition times. Notably, a major contribution to the discrepancy observed for the TPE/3MBD ratio calculated by ^1H NMR and ^{13}C NMR spectra could be ascribed to the relatively low concentration of TPE and 3MBD in the samples, which makes the ^{13}C NMR signal integration critical.

In this work, UDEFT experiments were also instrumental in confirming the presence of the allene quaternary ammonium salt of triethylamine (*N,N,N*-triethyl-triphenylpropadienamium chloride, TTPAC; see Scheme S2 on page 10).

Notably, the sample that produced the spectrum in Figure S7 yielded, under comparable acquisition time, the spectrum shown in Figure S8 when a standard sequence was used, illustrating how the low S/N ratio makes the allene carbon resonance very difficult to detect.

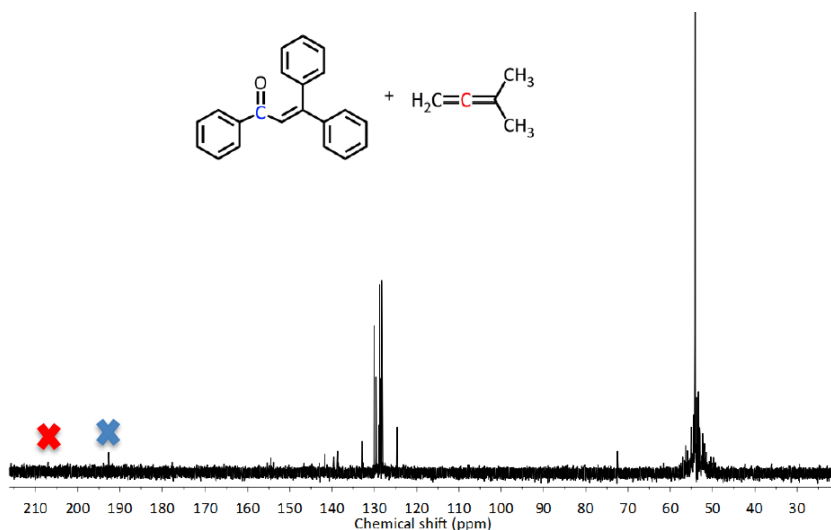


Figure S8. ^{13}C NMR (CD_2Cl_2 , 75 MHz) spectrum of TPE and 3MBD (22 and 43 mM respectively).

2.2 ^{13}C NMR UDEFT method for the characterization of reaction crudes

NMR samples for ^1H NMR and ^{13}C NMR UDEFT spectra collected in Section 5 were prepared introducing 500 μl of reaction crude and 200 μl of CD_2Cl_2 for locking. Each ^1H NMR spectrum was acquired with a zgpr sequence, which effects suppression of the solvent signal (CH_2Cl_2). The relaxation delay (D1) was set to 1 sec after every 90° pulse (7.8 μs). Each spectrum was acquired

with 8 scans. ^{13}C NMR spectra were acquired with UDEFT no NOE sequence (Figure S9), where the first pulse is a 90_{+x}° ($13\ \mu\text{s}$), followed by acquisition time of 360 ms. The next refocusing pulse was a 180_{+y}° (2 ms) adiabatic composite smoothed Chirp and the inversion pulse was a 180_{+x}° ($500\ \mu\text{s}$) adiabatic smoothed Chirp. The ^1H decoupling pulse employed is WALTZ 16. D1 was set to 3 s. Each spectrum was acquired with 1024 scans in 1 hour.

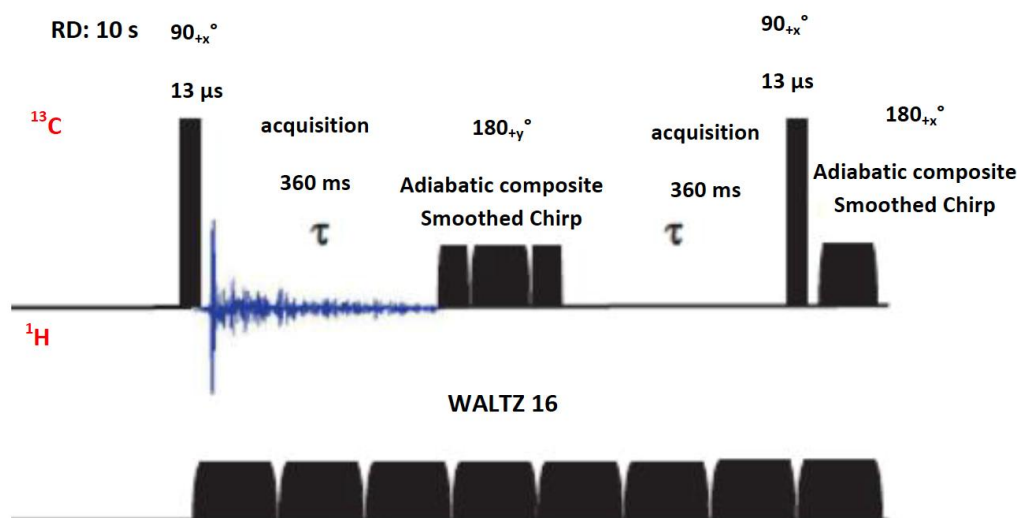


Figure S9. UDEFT no NOE sequence.

2.3. HPLC-MS method for the characterization of reaction crudes

HPLC analyses were performed using a Phenomenex Luna $5\ \mu\text{m}$ phenyl-hexyl column ($100 \times 4.6\ \text{mm}$) mounted on an Agilent 1100 Series pump system equipped with a diode-array UV detector and an Agilent G24450 APCI ionization source. A gradient elution was applied to improve the separation of TPPA, TPE, TPCA and coronene (used as internal standard). The gradient program (Table S1) enabled clear resolution of the first two compounds from the solvent front.

Time (min)	Acetonitrile %	Water %	Flow rate (ml/min)
0	70	30	1.0
6.5	70	30	1.0
9	95	5	1.0
25.0	95	5	1.0
30.0	70	30	1.0

Table S1. Gradient elution programme.

Retention times are collected in Table S2. Figure S10 reports the HPLC traces recorded from a solution of TPPA, TPE and coronene dissolved in CH_2Cl_2 . This test proves that TPPA and TPE can indeed be separated and identified by comparison with pure samples.

Compound	Retention time (min)
TPPA	8.1
TPE	10.2
TPCA	12.8
Coronene	13.8

Table S2. Standard samples retention times.

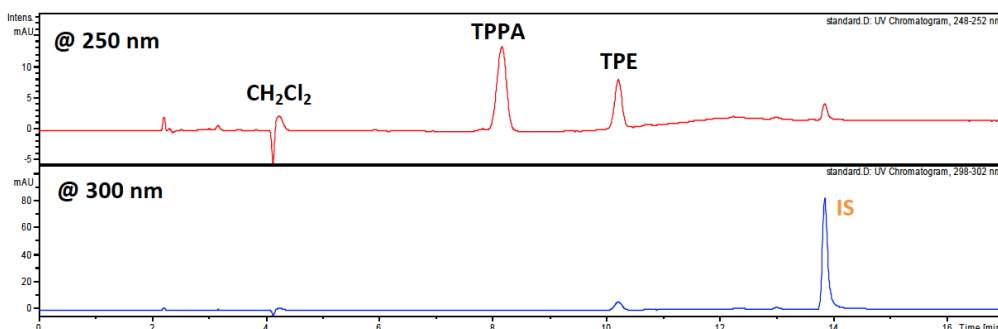
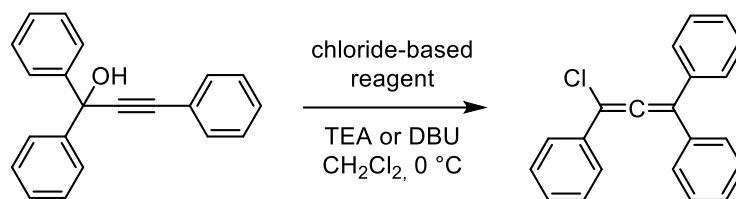


Figure S10. Elution of TPPA, TPE and internal standard (coronene) dissolved in CH_2Cl_2 .

2.4. Reaction of TPPA with different chloride-based reagents



The ^{13}C NMR UDEFT and HPLC-MS methods described above enabled us to compare different reactions and evaluate the performance of various chloride-based reagents. Comparisons were based on: (i) the amount of unreacted TPPA after 20 minutes at $0\text{ }^\circ\text{C}$; (ii) the yield of TPCA; and (iii) the formation of side products. A qualitative assessment of residual TPPA and the side product TPE was performed via HPLC by UV-Vis detection at 250 nm, where both compounds absorb, whereas the quantitative determination of TPCA relative to the coronene internal standard was carried out at 300 nm. For each reaction, the presence of TPCA and/or TPE was confirmed by examining the 190–210 ppm region of the ^{13}C NMR spectrum, where TPCA shows its allene carbon at 204 ppm and TPE displays its carbonyl carbon at 192 ppm. All ^{13}C NMR UDEFT spectra are collected in Section 5.

General Procedure. For each experiment, the chloride-based reagent (see Table S3 for exact quantities) was dissolved in anhydrous CH_2Cl_2 (4 ml) under a nitrogen atmosphere in an oven-dried 25 ml three-neck round-bottom flask equipped with a magnetic stirring bar. The solution was cooled to $0\text{ }^\circ\text{C}$ using an ice bath. Vilsmeier salt and triphenylphosphine dichloride were generated *in situ* from DMF/POCl_3 and PPh_3/BTC , respectively. A solution of TPPA (208.9 mg, 0.73 mmol, 1.0 equiv.) and base (1.79 mmol TEA or DBU, 2.5 equiv.), previously dissolved in anhydrous CH_2Cl_2 (1 ml), was added dropwise to the reaction flask. No base was used when employing triphenylphosphine dichloride. The reaction mixture was stirred for 20 minutes (or 60 minutes with triphenylphosphine dichloride, and 120 minutes for the Vilsmeier reagent), then monitored by HPLC-MS (APCI) and by ^{13}C NMR.

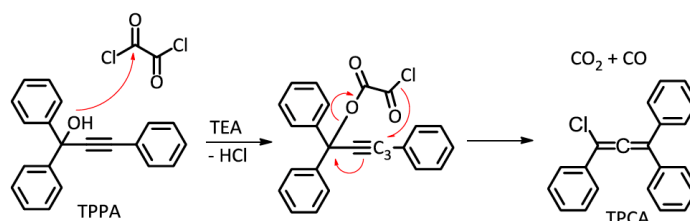
HPLC-MS Sample Preparation. Fifty microlitres of the crude mixture were diluted in 5 ml of CH_2Cl_2 and washed with saturated sodium bicarbonate. The organic phase was filtered through a $0.2\text{ }\mu\text{m}$ PTFE membrane. An aliquot of 100 μl of the filtrate was diluted in 2 ml of HPLC-grade acetonitrile together with 50 μl of the internal standard solution. The sample was analysed using the elution method described in Table S1.

NMR Sample Preparation. For NMR analysis, 500 μl of the crude mixture were transferred into a screw-cap NMR tube, then 200 μl of CD_2Cl_2 were added to provide a lock signal.

Solvent	Reagent	Equivalents	Weight (mg)	Volume (ml)	moles (mmol)	Concentration (mM)
CH ₂ Cl ₂ (5 ml)	TPPA	1.0	208.2		0.73	137.2
	OxCl	1.1		0.07	0.81	152.2
	TEA	2.5		0.25	1.79	336.5
	TPPA	1.0	205.8		0.72	135.3
	MesCl	1.3		0.07	0.90	169.2
	TEA	2.5		0.25	1.79	336.4
	TPPA	1.0	205.8		0.73	136.7
	MesCl	1.3		0.07	0.90	168.5
	DBU	2.6		0.27	1.90	355.8
	TPPA	1.0	208.9		0.73	139.0
	PCl ₅	1.3	197.3		0.95	181.0
	TEA	2.5		0.25	1.79	341.0
	TPPA	1.0	208.9		0.73	138.5
	PCl ₅	1.3	197.3		0.95	180.3
DBU	2.5		0.27	1.90	360.5	
TPPA	1.0	196.4		0.69	127.5	
DMF	1.2		0.08	1.03	190.4	
POCl ₃	1.4		0.08	0.86	159.0	
TEA	2.6		0.25	1.79	330.9	
TPPA	1.0	219.9		0.77	154.0	
PPh ₃	1.27	257.7		0.98	196.0	
BTC	1.27	97.4		0.98	196.0	

Table S3. Reaction conditions for TPPA halogenation with different chloride-based reagents.

2.4.1 Oxalyl chloride (base: TEA)



The HPLC trace in Figure S11 shows complete conversion of TPPA. No TPE is detected (expected retention time: 10.2 min), and only TPCA appears at 12.8 min in addition to the internal standard. The ratio between these two chromatographic peaks is 0.58.

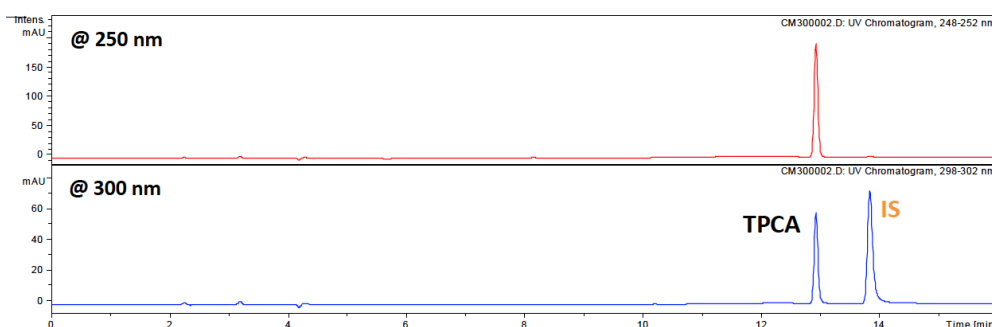


Figure S11. HPLC-MS (APCI) trace of the crude reaction mixture obtained from the reaction of TPPA with oxalyl chloride and TEA.

In the ¹³C NMR UDEFT spectrum (UDEFT_1) TPCA gives its expected signals at 203.8 ppm (allene carbon), 119.5 and 108.1 ppm (sp² carbons in the propadiene moiety). Weak signals from the propargyl carbons of TPPA are also present, at 92.6 and 86.2 ppm, indicating that TPPA traces are still present in the mixture, albeit undetected by the HPLC assay. Furthermore, no signal was detected for the carbonyl carbon of TPE (192.0 ppm).

2.4.2 Methanesulfonyl chloride (base: TEA and DBU)

The reaction of TPPA with methanesulfonyl chloride (MsCl, see Scheme 2 in the manuscript for the mechanism) and TEA proceeded quickly, as TLC analysis showed a complete conversion of TPPA in less than 20 min at 0 °C. The crude mixture appeared pale orange, with no visible precipitation of salts. The HPLC chromatogram reported in Figure S12 displays traces of TPPA (8.0 min) and confirms the absence of TPE. The ratio between the integrals of the TPCA peak and the internal standard at 300 nm is 0.29.

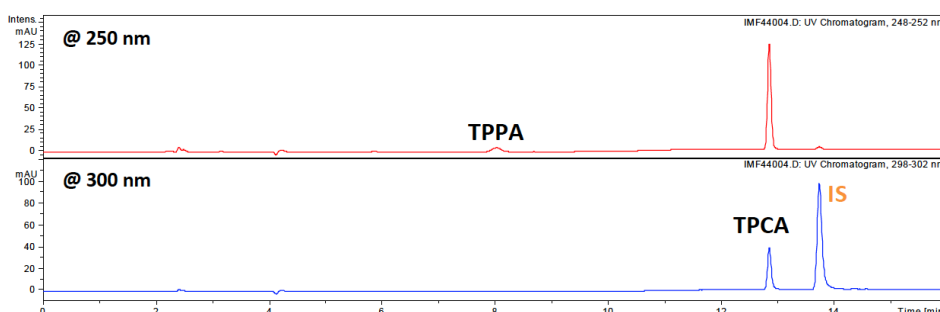
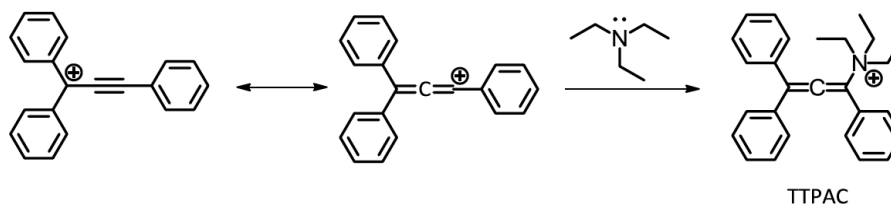


Figure S12. HPLC-MS (APCI) trace of the crude reaction mixture obtained from the reaction of TPPA with MsCl and TEA.

In the ¹³C NMR UDEFT spectrum (UDEFT_2), the signals of methanesulfonic acid (39.4 ppm) and TEA (45.6 ppm) are clearly observed. The absence of the two propargyl carbon resonances of TPPA (92.2 and 85.5 ppm), together with the lack of the MsCl signal at 50.5 ppm, indicates that chlorination proceeded to completion. No resonance attributable to the carbonyl carbon of TPE is detected

around 192 ppm. Instead, two signals appear at 200.3 and 203.8 ppm, accompanied by two sets of resonances at 108.0–119.5 ppm and 115.2–121.8 ppm, assignable to the peripheral carbons of two distinct propadiene systems. The signal at 203.8 ppm is attributed to TPCA, whereas the resonance at 200.3 ppm matches the literature value for the TTPAC.



Scheme S2. Formation of TTPAC.

To corroborate the mechanism proposed in Scheme S2, the reaction was repeated using DBU in place of TEA. The change of base slowed down the reaction, and the HPLC trace recorded at 250 nm (Figure S13) shows the presence of unreacted alcohol. DBU is a strong organic base with weak nucleophilicity, consistently, the signal at 200.3 ppm is completely absent in the resulting ^{13}C NMR UDEFT spectrum (UDEFT_3). In addition, the ratio between the integrals of the TPCA and internal standard peaks detected at 300 nm increases to 0.41.

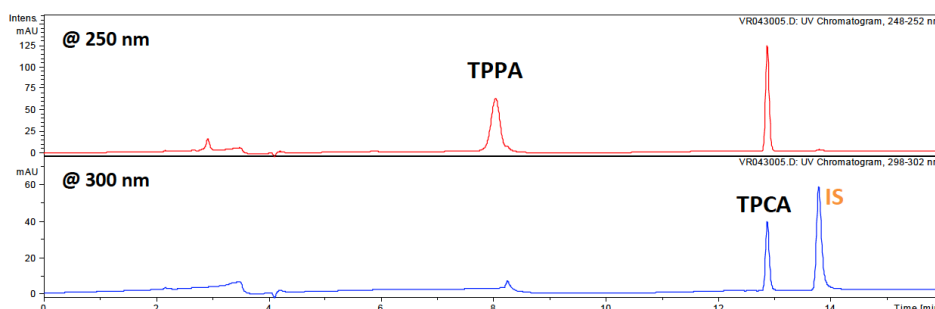
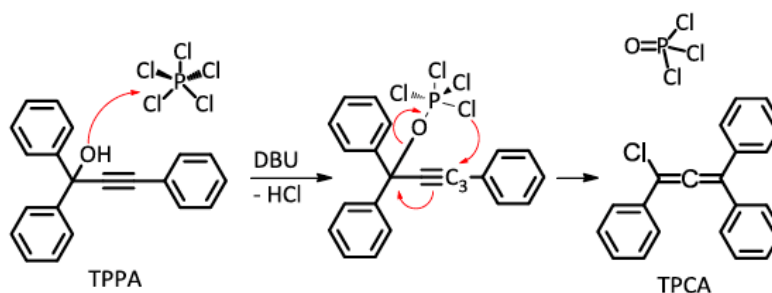


Figure S13. HPLC-MS (APCI) trace of the crude reaction mixture obtained from the reaction of TPPA with MsCl and DBU.

2.4.3 Phosphorus pentachloride (base: TEA and DBU)



After 20 minutes of reaction, the crude mixture appeared as a clear, pale-yellow solution.

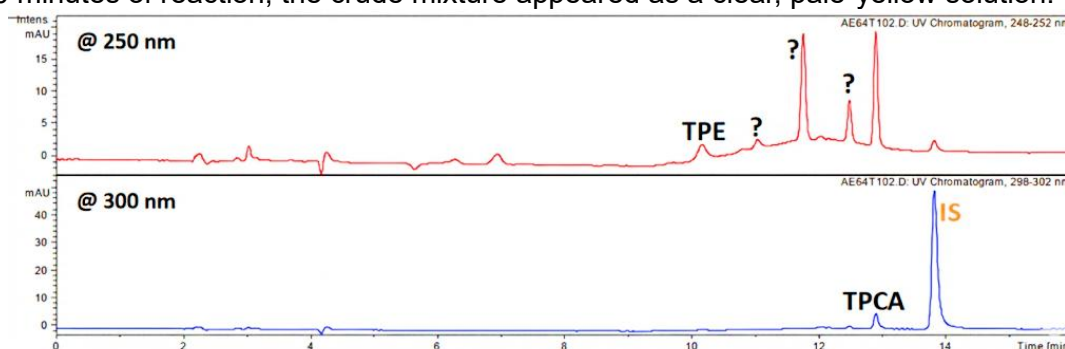


Figure S14. HPLC-MS (APCI) trace of the crude reaction mixture obtained from the reaction of TPPA with PCl_5 and TEA.

PCl_5 -mediated activation shows a marked dependence on the base employed. When triethylamine is used as the base, only limited TPCA formation is observed, whereas significantly higher yields are obtained in the presence of DBU (Table 1 in the main text), consistent with a more efficient generation of the activated propargylic intermediate promoted by the stronger base. Under these conditions, the solubility of the corresponding base hydrochloride in the employed reaction medium suggests that chloride availability may no longer be fully suppressed, complicating a strict mechanistic assignment.

As shown in Figure S14, at 250 nm, only residual traces of TPE are detected at 10.2 min. The chromatogram also displays the peak of TPCA at 12.8 min, along with the internal standard at 13.8 min, and several additional, unidentified components. TPPA was almost completely consumed under these conditions. The ratio between the chromatographic peak areas of TPCA and the internal standard is approximately 0.11. The UDEFT ^{13}C NMR spectrum (UDEFT_4) does not show the resonance at 192 ppm, typical of TPE, which was detected only in trace amounts by HPLC. It is worth noting that TPE may have formed during the workup of the crude mixture prior to HPLC injection. Weak signals attributable to the propargyl carbons of TPPA were observed at 85.5 and 92.2 ppm. Notably, no allene carbon resonance was detected at 203.8 ppm, whereas the two expected signals for the other TPCA carbons were observed at 109.0 and 119.5 ppm. As suggested by the HPLC analysis, TPCA may have been produced in quantities so small that the slowly relaxing allene carbon signal remained below the noise threshold in the ^{13}C NMR experiment. As in the case of MsCl , the reaction with PCl_5 was carried out using DBU as base. The HPLC chromatograms of the crude mixture are shown in Figure S15.

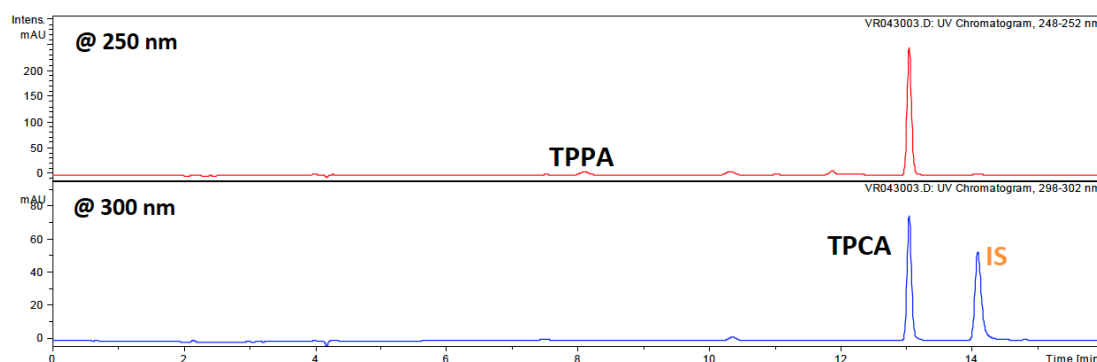
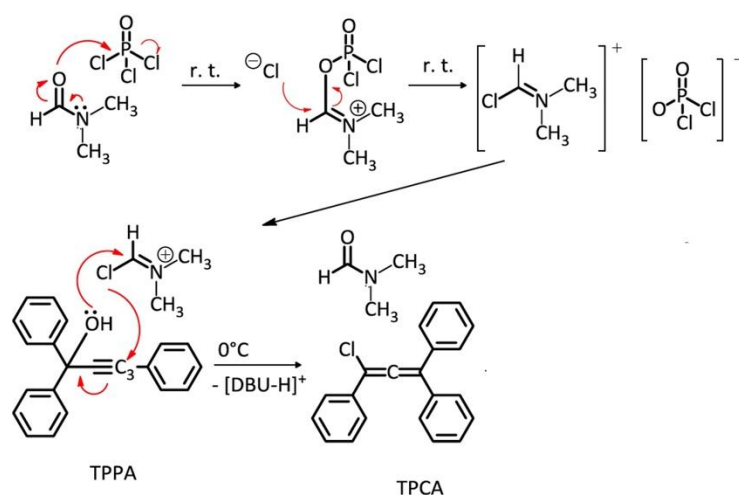


Figure S15. HPLC-MS (APCI) trace of the crude reaction mixture obtained from the reaction of TPPA with PCl_5 and DBU.

The chromatograms were considerably clean, with few unassigned peaks and only traces of side products. The TPCA/internal standard ratio amounted to 0.85, with a traces presence of TPPA. Moreover, the ^{13}C NMR spectrum (UDEFT_5) only show the signal at 203.8 ppm for TPCA, confirming that TTPAC was not produced.

2.4.4 Vilsmeier reagent (base: TEA)

Chloromethylene dimethyliminium chloride, commonly known as the Vilsmeier reagent, is an intramolecular reagent used for the conversion of alcohols into the corresponding chlorides. Its reactivity toward nucleophiles arises from the strong electrophilic character of the iminium carbon, which also makes the reagent intrinsically unstable. It must therefore be stored at low temperature and used within a few days of opening the container. For this reason, in this study the Vilsmeier reagent was generated *in situ* from *N,N*-dimethylformamide and phosphoryl chloride (POCl_3), as shown in Scheme S3, along with its reaction with TPPA.



Scheme S3. Synthesis of the Vilsmeier reagent and its reaction with TPPA.

The HPLC traces in Figure S16 correspond to the reaction crude after 120 minutes at 0 °C. The reaction proceeded cleanly, with no detectable side products. The chromatogram shows TPPA (8.1 min) and TPCA (12.9 min), and the TPCA/Internal standard ratio is 0.20. Overall, the transformation is noticeably slower than the other reactions studied in this work.

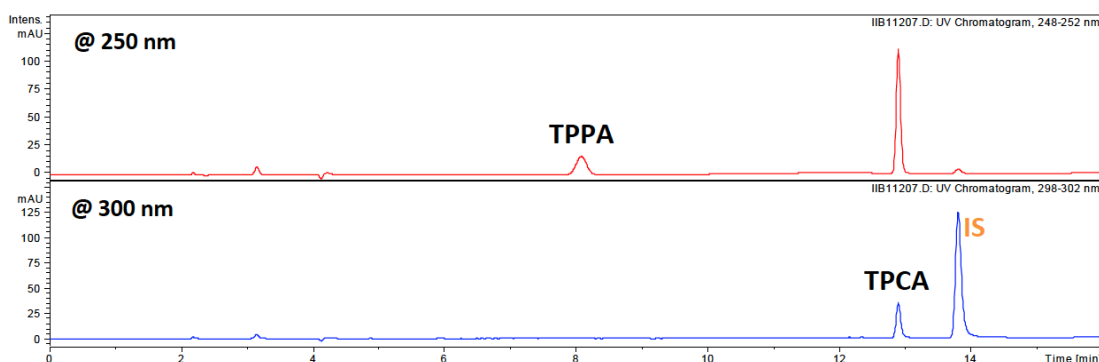


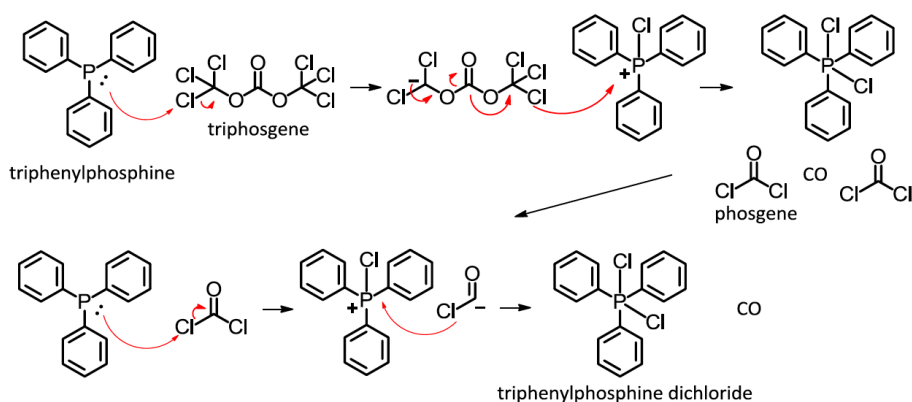
Figure S16. HPLC-MS (APCI) trace of the crude reaction mixture obtained from the reaction of TPPA with the Vilsmeier reagent and TEA.

The ¹³C NMR UDEFT spectrum (UDEFT_6) confirms the presence of unreacted TPPA, with propargyl carbons resonating at 92.3 and 86.6 ppm. Signals at 36.2 and 30.6 ppm correspond to the methyl groups of *N,N*-dimethylformamide, while the aldehydic carbon appears at 162.2 ppm. Despite the reasonable conversion of TPPA, only a weak signal at 200.3 ppm, likely associated with TTPAC, is observed. The resonances of the sp² carbons of the propadiene system are also absent in the 120-110 ppm region.

Given its slower kinetics compared to the other chlorinating systems, this reaction is less attractive for potential implementation toward the synthesis of rubrene.

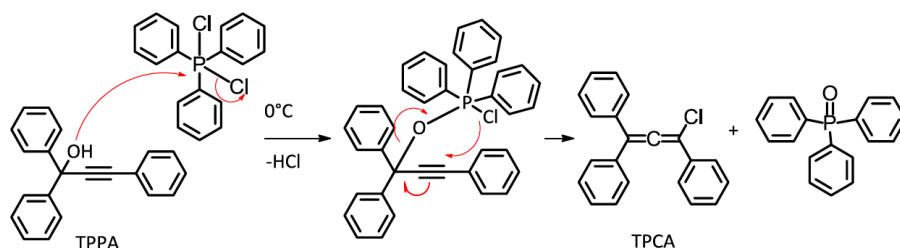
2.4.5 Triphenylphosphine dichloride

Triphenylphosphine dichloride was generated *in situ* by treatment of triphenylphosphine with triphosgene. The proposed mechanism for the formation of triphenylphosphine dichloride is reported in Scheme S4.



Scheme S4. Formation of PPh_3Cl_2 .

The proposed mechanism for the reaction of PPh_3Cl_2 with TPPA is shown in Scheme S5. The electrophilic phosphorus atom of triphenylphosphine is first attacked by the hydroxyl group of TPPA, generating a triphenylphosphine chloride intermediate and releasing HCl . The chloride then performs an intramolecular attack on the β -propargyl carbon of this intermediate, affording TPCA along with triphenylphosphine oxide. The strong thermodynamic driving force for the reaction is the formation of the $\text{P}=\text{O}$ bond.



Scheme S5. Reaction of PPh_3Cl_2 with TPPA.

The chromatogram in Figure S17 was recorded after extending the reaction time to 60 minutes. A substantial amount of unconverted TPPA (peak at 8.4 min) is still clearly visible in the HPLC trace at 250 nm. Besides the starting material, only trace amounts of TPE appear at 10.4 min, along with TPCA, whose peak area corresponds to a TPCA/internal standard ratio of 0.12. Overall, the HPLC analysis indicates a clean yet slow reaction, with no detectable side products.

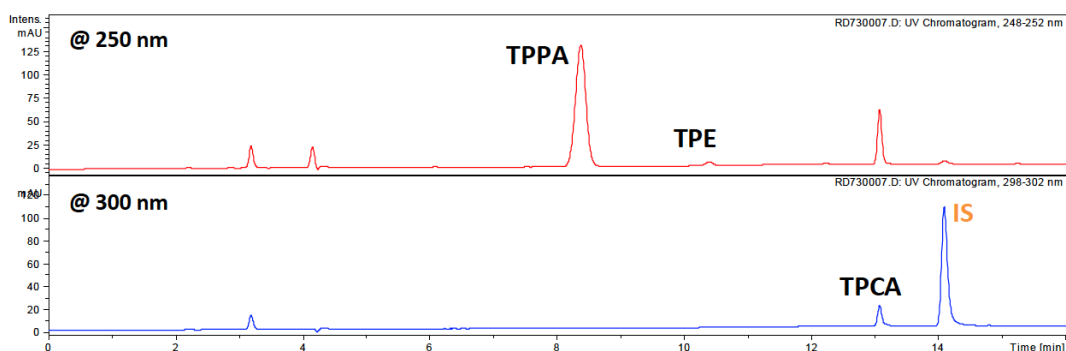


Figure S17. HPLC-MS (APCI) trace of the crude reaction mixture obtained from the reaction of TPPA with PPh_3Cl_2 .

In this case, ^{13}C NMR UDEFT analysis of the crude mixture were not performed due to dielectric de-matching effects in the sample. In any case, the reaction proceeded too slowly to warrant further investigation in this study.

3. Optimization of the one-pot synthesis of rubrene

3.1. Determination of rubrene concentration by UV-Vis spectroscopy

UV-Vis spectroscopy was used to obtain a preliminary estimate of reaction yields (UV-Vis yields), exploiting the characteristic absorption profile of rubrene, which exhibits a set of bands in the visible region (400-550 nm) with a maximum at 527 nm. Aliquots (a few microlitres) were withdrawn from the reaction mixtures, diluted with toluene in volumetric flasks, filtered through 0.22 μm syringe filters to remove undissolved materials (e.g., hydrochloride salts), and then analysed.

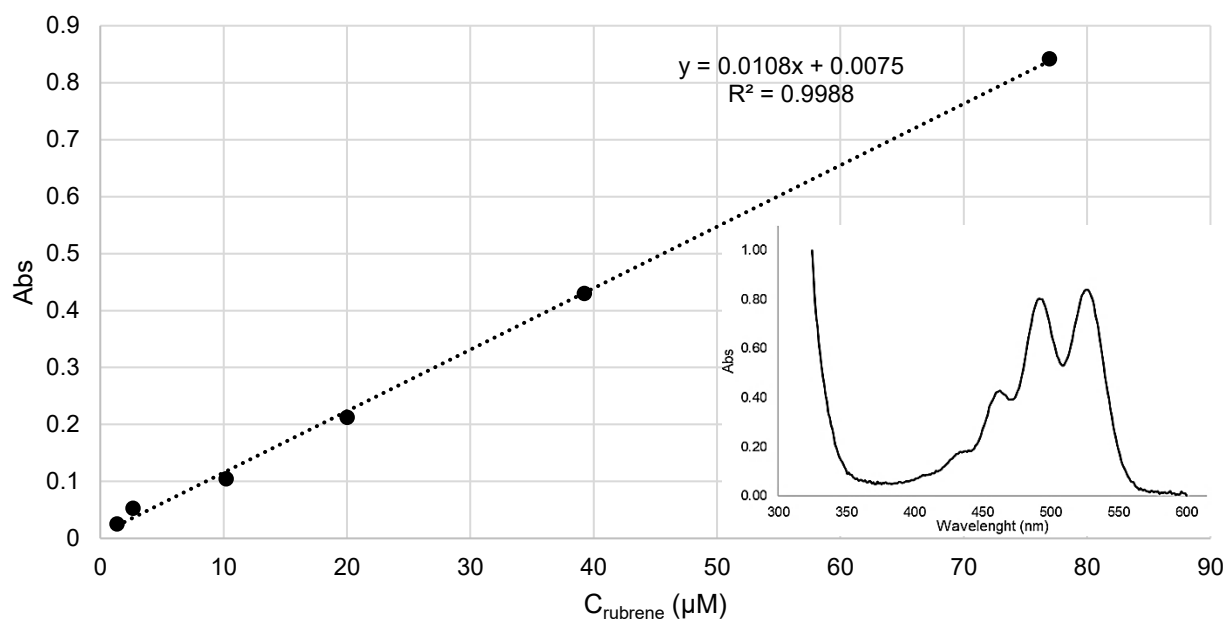


Figure S18. UV-Vis calibration curve for rubrene in toluene (1-80 μM), recorded at $\lambda = 527$ nm. Inset: UV-Vis spectrum of the rubrene standard.

3.2. Synthesis of rubrene with PCl_5 : reaction conditions screening

Optimization of the PCl_5 reaction for the synthesis of rubrene, conventional heating

Rubrene synthesis using PCl_5 was examined as a function of temperature (120, 140, and 150 °C) and initial TPPA concentration ($C_{\text{TPPA}}^i = 0.05, 0.10,$ and 0.20 M) in *o*-dichlorobenzene (ODCB) as solvent. In all cases, rubrene formation increased linearly with time, with higher temperatures leading to faster reaction rates. TPPA concentrations below 0.10 M markedly reduced the formation rate, whereas increasing C_{TPPA}^i above 0.10 M did not provide further kinetic benefit, indicating an optimal concentration under these conditions. Prolonged heating at 140 °C (17 h, $C_{\text{TPPA}}^i = 0.10$ M) afforded a **45% UV-Vis yield** of rubrene while reactions at 150 °C with $C_{\text{TPPA}}^i = 0.10$ and 0.20 M resulted in lower rubrene yields (**37%** and **39%**, **UV-Vis yield** respectively).

General procedure. PCl_5 (189 mg, 0.91 mmol, 1.3 equiv.) was dissolved in ODCB (1.5, 5.0, or 12 ml to achieve $C_{\text{TPPA}}^i = 0.20, 0.10$ or 0.05 M, respectively) under a nitrogen atmosphere. The mixture was cooled to 0 °C, and a (2 ml, ODCB) solution of TPPA (200 mg, 0.70 mmol, 1.0 equiv.) was added dropwise. After stirring for 30 min, DBU (350 μl , 2.34 mmol, 3.3 equiv.) was added, and the mixture was heated at the selected temperature for 5 h. Reaction progress was monitored by UV-Vis spectroscopy.

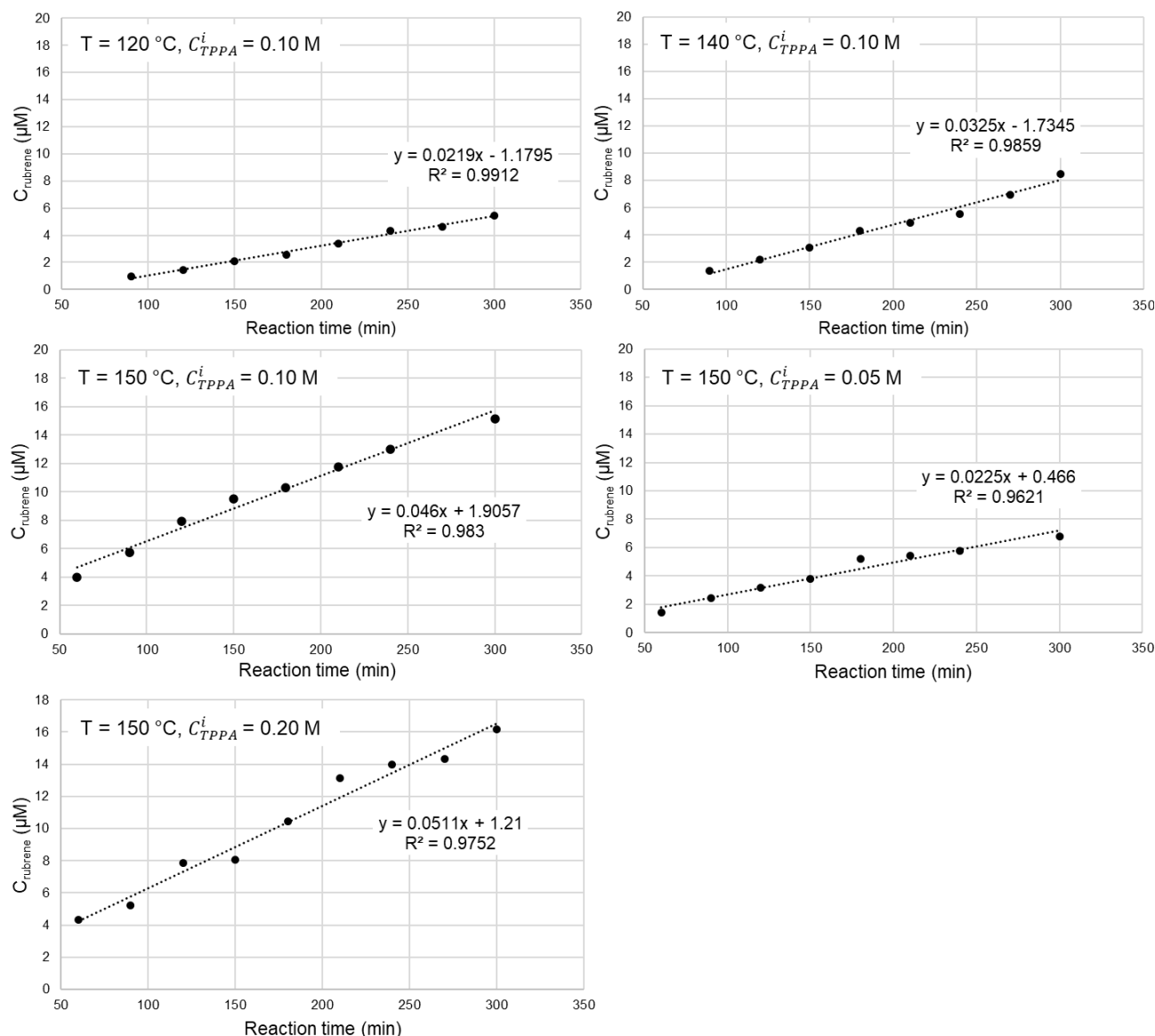


Figure S19. Reaction condition screening for rubrene synthesis under conventional heating.

Selected procedure for rubrene synthesis using PCl_5 under conventional heating (M1). In a thick-walled screw-cap sealed glass tube, PCl_5 (66 mg, 317 μmol , 1.3 equiv.) was dissolved in ODCB (1.7 ml) under a nitrogen atmosphere. The stirred solution was cooled to 0 °C, and a solution of TPPA (68.5 mg, 241 μmol , 1.0 equiv.) in ODCB (1.0 ml) was added dropwise. The mixture was stirred at 0 °C for 30 min, after which collidine (160 μl , 1.21 mmol, 5.0 equiv.) was added dropwise. The tube was rapidly sealed and heated at 140 °C in an oil bath for 24 h. After cooling to room temperature, the reaction mixture was diluted with toluene and concentrated under reduced pressure. The residue was triturated with MeOH (20 ml), vacuum-filtered through a Hirsch funnel, and washed with MeOH (3 \times 10 ml). The solid was dried under vacuum and purified by column chromatography on neutral activated alumina (petroleum ether) to afford rubrene as an orange-red powder (31 mg, 58.2 μmol , **48% yield**).

Optimization of the PCl_5 reaction for the synthesis of rubrene under microwave heating

The microwave-assisted synthesis of rubrene using PCl_5 was examined over a range of temperatures and reaction times (Figure S20). Within the explored time window, 160 °C afforded the highest yields. At 140 °C, rubrene formation proceeded more slowly, whereas at 180 °C the yield reached a maximum after 60 min and then decreased, likely due to high-temperature-induced side reactions (see procedure M2 reported below)

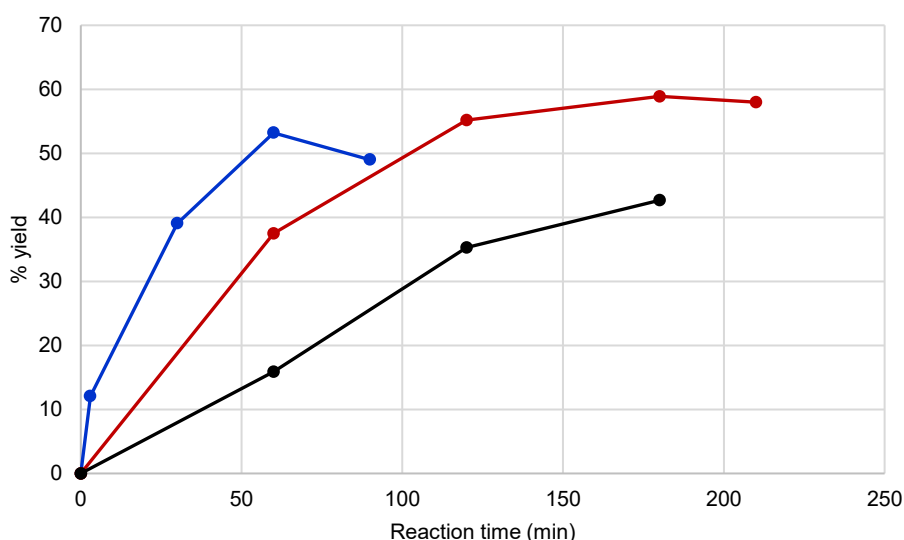


Figure S20. Time-dependent UV-Vis yields for rubrene synthesis using PCl_5 under microwave heating at 140 (•), 160 (•), and 180 (•) °C.

Selected procedure for rubrene synthesis using PCl_5 under microwave heating (M2). In a thick-walled screw-cap sealed glass tube, PCl_5 (66 mg, 317 μmol , 1.3 equiv.) was dissolved in ODCB (1.7 ml) under a nitrogen atmosphere and cooled to 0 °C. A solution of TPPA (68.5 mg, 241 μmol , 1.0 equiv.) in ODCB (1.0 ml) was added dropwise, and the mixture was stirred at 0 °C for 30 min. Collidine (160 μl , 1.21 mmol, 5.0 equiv.) was then added dropwise, the tube sealed, and the reaction heated under microwave irradiation at 160 °C for 3 h. After cooling to room temperature, the mixture was diluted with toluene and concentrated under reduced pressure. The residue was triturated with MeOH (20 ml), vacuum-filtered, and washed with MeOH (3 \times 10 ml). Purification by column chromatography on neutral activated alumina (petroleum ether) afforded rubrene as an orange red powder (25 mg, 46.9 μmol , **38% yield**).

3.3 Synthesis of rubrene with TMSCI

Optimization of the TMSCI reaction for the synthesis of rubrene

The TMSCI-mediated synthesis of rubrene was initially optimised by varying the equivalents of TMSCI and 2,6-di-*tert*-butylpyridine (DTBP), as summarised in Table S4 (**entries 1–6**). Reactions were conducted under nitrogen in a thick-walled, screw-cap sealed glass tube using ODCB (1 ml) as solvent. After 8 h, aliquots were analysed by UV-Vis spectroscopy to determine the yield. Extending the reaction time to 16 h did not result in further yield improvement. Among the conditions examined, 1.1 equiv. of TMSCI and 3.0 equiv. of DTBP provided the highest UV-Vis yield (66%). An exploratory experiment performed at doubled TPPA concentration (**entry 7, Table S4**) afforded a comparable UV-Vis yield (69%). Under these latter conditions, scale-up of the reaction delivered rubrene in 68% UV-Vis yield (**entry 8, Table S4**). These conditions were therefore selected as the optimal ones (M3).

Entry	TMSCI (equiv.)	DTBP (equiv.)	UV-Vis yield
1 ^a	1.5	3.0	57%
2 ^a	1.5	2.0	47%
3 ^a	1.0	3.0	55%
4 ^a	3.0	3.0	26%
5 ^a	1.0	2.0	54%
6^a	1.1	3.0	66%
7^b	1.1	3.0	69%
8^c	1.1	3.0	68%

Table S4. TMSCI-based rubrene synthesis optimisation: screening of TMSCI and DTBP equivalents in ODCB at 140 °C for 8h.

^a $m_{TPPA}^i = 68.5 \text{ mg}$, $C_{TPPA}^i = 203 \text{ mM}$

^b $m_{TPPA}^i = 127.0 \text{ mg}$, $C_{TPPA}^i = 406 \text{ mM}$

^c $m_{TPPA}^i = 1.0 \text{ g}$, $C_{TPPA}^i = 406 \text{ mM}$

Optimised procedure for the scale-up of rubrene synthesis using TMSCI under conventional heating (M3). In a thick-walled screw-cap sealed glass tube, TPPA (1.0 g, 3.52 mmol, 1.0 equiv.) was dissolved in ODCB (4.6 ml). Under a nitrogen atmosphere, DTBP (2.28 mL, 10.56 mmol, 3.0 equiv.) and TMSCI (482 μ l, 3.87 mmol, 1.1 equiv.) were added sequentially at room temperature. The tube was sealed and the reaction stirred at 140 °C for 8 h. After cooling to room temperature, the mixture was diluted with toluene and concentrated under reduced pressure. The residue was triturated with MeOH (50 ml), vacuum-filtered, and washed with MeOH (3 \times 10 ml) to afford pure rubrene as an orange–red powder (571 mg, 1.08 mmol, **61% yield**).

3.4 NMR yield quantification of rubrene (PCl_5 , conventional heating - M1)

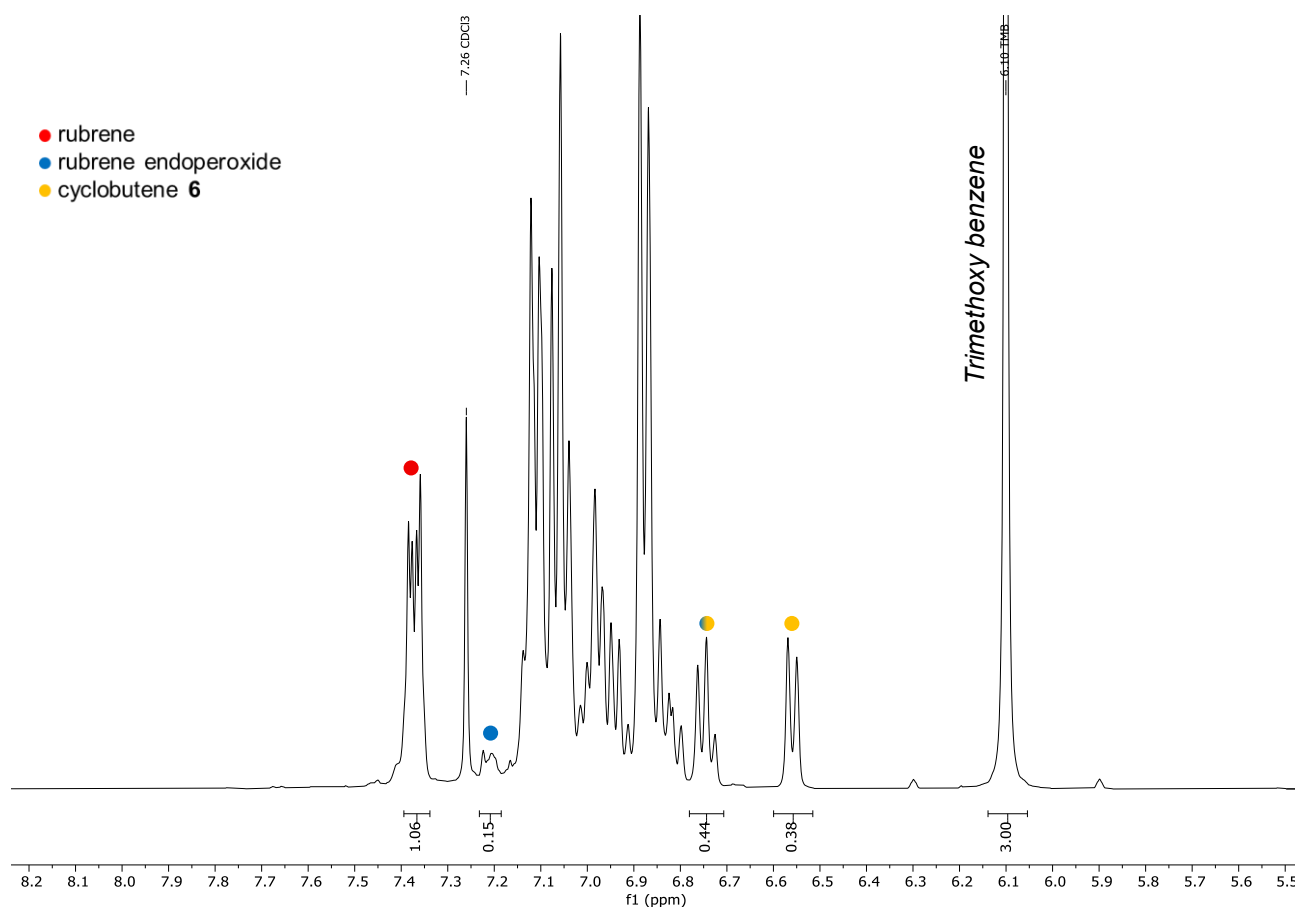


Figure S21. ^1H NMR (500 MHz, CDCl_3) spectrum of the crude reaction mixture obtained from rubrene synthesis with PCl_5 after evaporation of ODCB, MeOH trituration and filtration (method M1, see above) using conventional heating at 140 °C overnight. 1,3,5-Trimethoxybenzene was used as the internal standard for quantitative analysis. The identified components were rubrene, cyclobutene **6**, and trace amounts of rubrene endoperoxide (rubrene:cyclobutene ratio of 2.8:1, see Table S5).

compd	δ (ppm)	Integration	Calc. weights	NMR yield
Rubrene	7.39	1.06 (4H)	35.8 mg (67.20 μmol)	56% (62%) ^a
Endoperoxide	7.23 6.77	0.15 (6H) (0.44-0.38) = 0.06 (2H)	4.2 mg (7.44 μmol)	6%
Cyclobutene 6	6.58	0.38 (4H)	12.9 mg (24.13 μmol)	20%

^a Sum of the yields of rubrene and rubrene endoperoxide.

^b The signal at 6.77 ppm (A) arises from the overlap of a rubrene endoperoxide resonance (B, 2H) and that of a cyclobutene resonance (C, 4H). Since the cyclobutene contribution (C) integrates identically to the signal at 6.58 ppm (D, 4H), the endoperoxide contribution was calculated using the relation $\mathbf{B} = \mathbf{A} - \mathbf{C}$, with $\mathbf{C} = \mathbf{D}$

Table S5. Integrated peak areas and NMR-based yield determination of the species present in the crude reaction mixture (method M1, see spectrum in Figure S21). The internal standard 1,3,5-Trimethoxybenzene (42.5 mg, 252.69 μmol) was added to a CDCl_3 solution of the crude reaction mixture, which was directly analysed by ^1H NMR. Integration of diagnostic signals of the species present and comparison with the trimethoxybenzene singlet (δ 6.10 ppm, 3H) enabled the quantification of rubrene, rubrene endoperoxide, and cyclobutene **6** in mmol, and the calculation of the corresponding yields.

3.5 NMR yield quantification of rubrene (PCl_5 , microwave heating - M2)

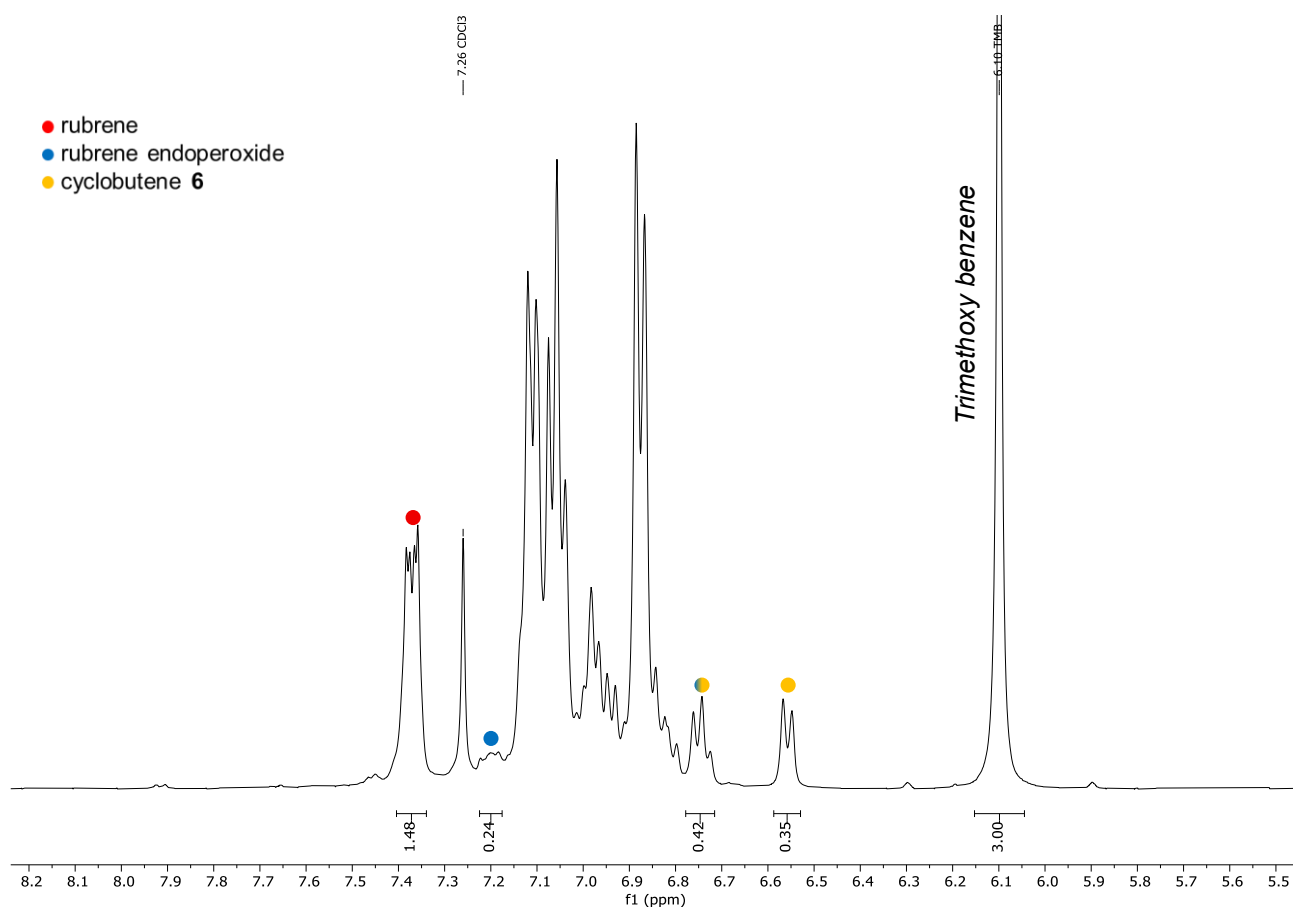


Figure S22. ^1H NMR (500 MHz, CDCl_3) spectrum of the crude reaction mixture obtained from rubrene synthesis with PCl_5 after evaporation of ODCB, MeOH trituration and filtration (method M2, see above) using microwave heating at 160 °C for 3h. 1,3,5-Trimethoxybenzene was used as the internal standard for quantitative analysis. The identified components were rubrene, cyclobutene **6**, and trace amounts of rubrene endoperoxide (rubrene:cyclobutene ratio of 4.2:1, see Table S6).

cmpd	δ (ppm)	Integration	Calc. weights	NMR yield
Rubrene	7.39	1.48(4H)	36.6 mg (68.71 μmol)	57% (62%) ^a
Endoperoxide	7.23 6.77	0.24 (6H) (0.42-0.35) = 0.07 (2H) ^b	3.74 mg (6.62 μmol)	5%
Cyclobutene 6	6.58	0.35 (4H)	8.78 mg (16.42 μmol)	14%

^a Sum of the yields of rubrene and rubrene endoperoxide.

^b The signal at 6.77 ppm (A) arises from the overlap of a rubrene endoperoxide resonance (B, 2H) and that of a cyclobutene resonance (C, 4H). Since the cyclobutene contribution (C) integrates identically to the signal at 6.58 ppm (D, 4H), the endoperoxide contribution was calculated using the relation $\mathbf{B} = \mathbf{A} - \mathbf{C}$, with $\mathbf{C} = \mathbf{D}$.

Table S6. Integrated peak areas and NMR-based yield determination of the species present in the crude reaction mixture (method M2, see spectrum in Figure S22). The internal standard 1,3,5-Trimethoxybenzene (31.3 mg, 186.1 μmol) was added to a CDCl_3 solution of the crude mixture, which was directly analysed by ^1H NMR. Integration of diagnostic signals of the species present and comparison with the trimethoxybenzene singlet (δ 6.10 ppm, 3H) enabled the quantification of rubrene, rubrene endoperoxide, and cyclobutene **6** in mmol, and the calculation of the corresponding yields.

3.6 NMR of rubrene (exp. 6, Table S4)

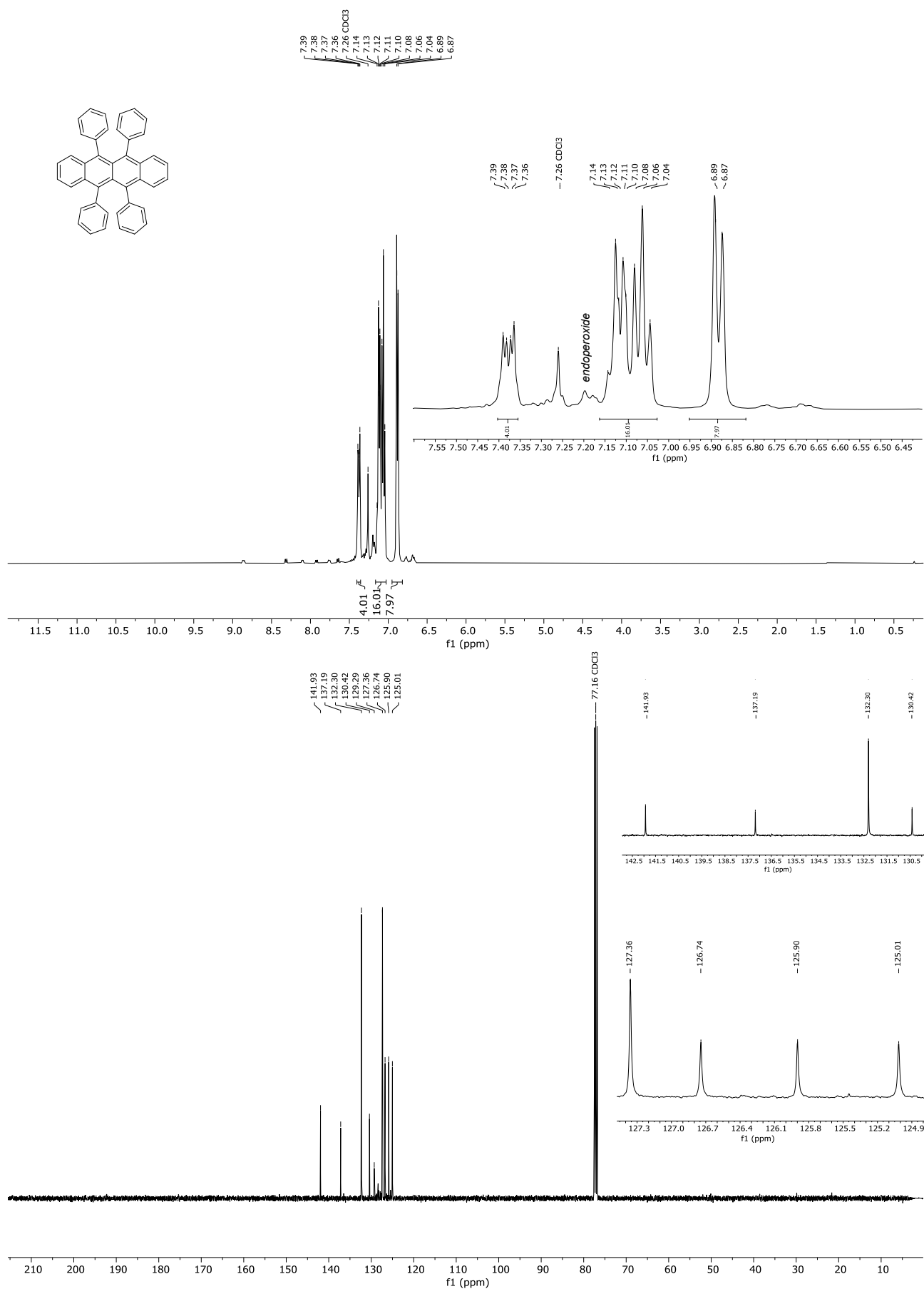


Figure S23. ^1H NMR (500 MHz, CDCl_3) and ^{13}C NMR (125 MHz, CDCl_3) spectra of rubrene (entry 6, table S4).

3.7 ¹H NMR of rubrene from the scale-up experiment (TMSCl, conventional heating - M3)

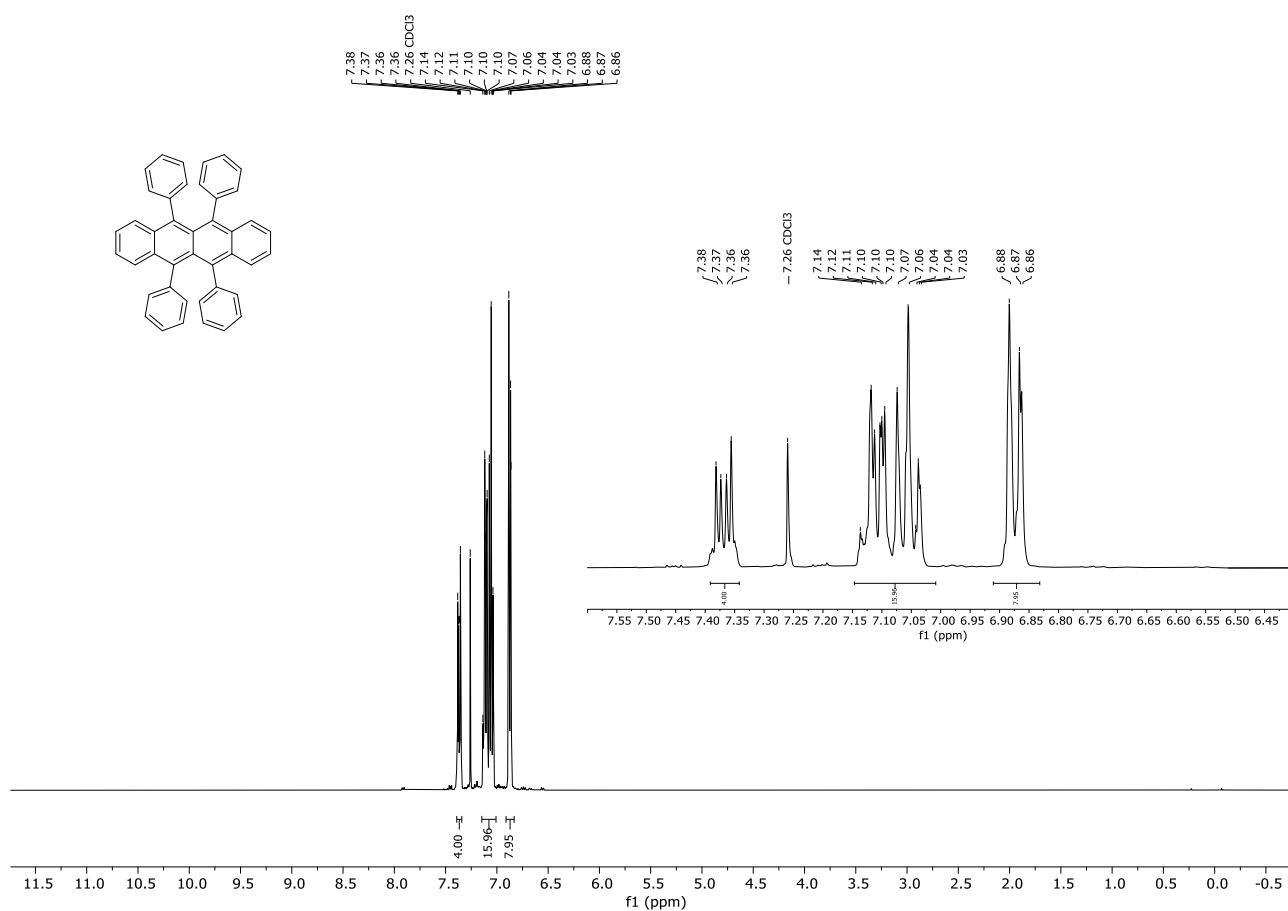


Figure S24. ¹H NMR (500 MHz, CDCl₃) spectrum of rubrene (entry 8, table S4).

3.8 NMR MR and UPLC-HRMS analysis of TPE (exp. 6, Table S4)

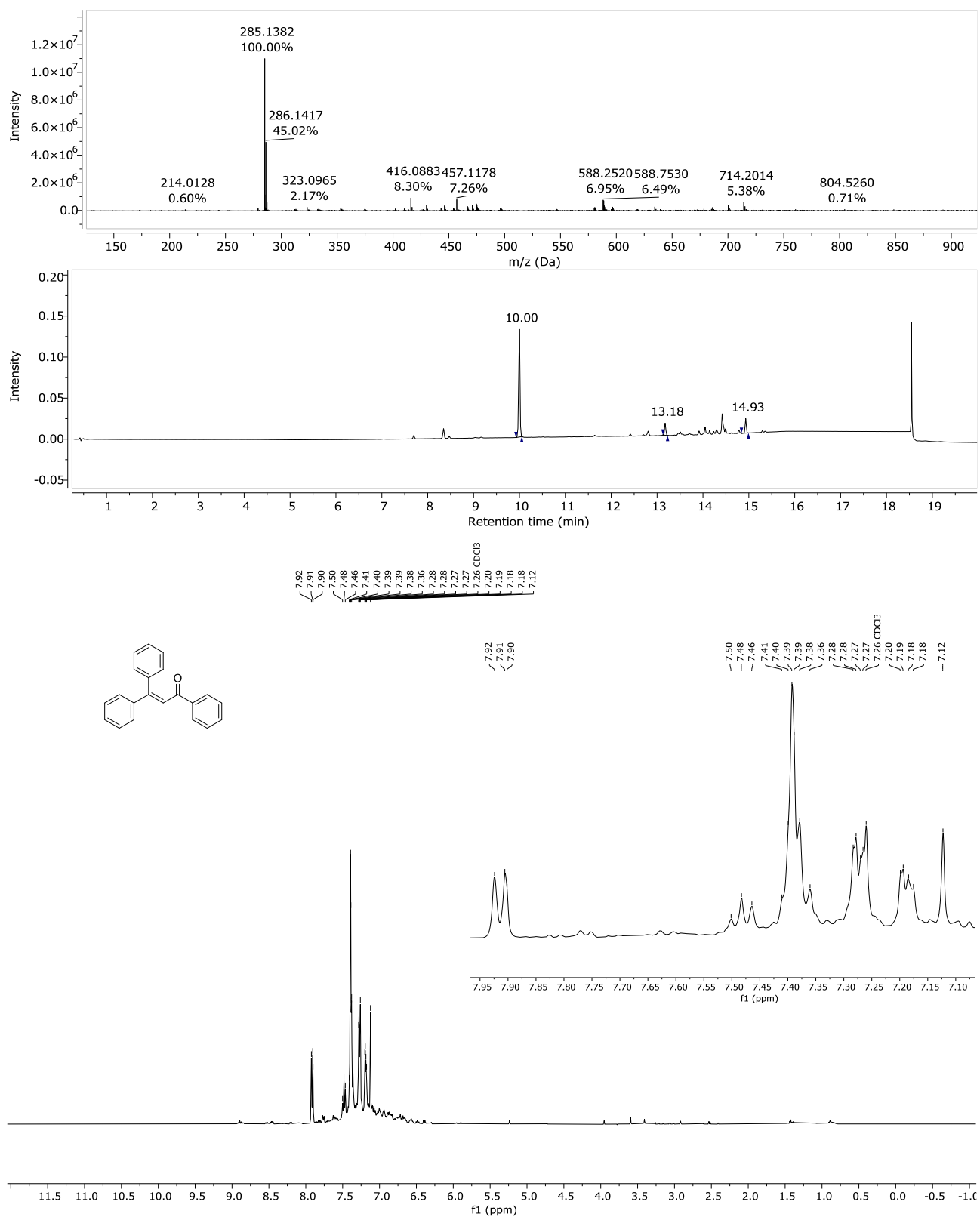


Figure S25. UPLC-HRMS and ¹H NMR (500 MHz, CDCl₃) analysis of the methanol filtrate obtained from the rubrene synthesis performed according to the conditions of experiment 6 indicated in Table S4. Chromatographic analysis showed TPE (10 min) as the major component, with trace amounts of rubrene endoperoxide (13.18 min) and rubrene (14.93 min). Additional minor peaks were detected but not identified due to their low responsiveness under ESI ionization conditions. This composition was subsequently confirmed by ¹H NMR spectroscopy, which also identified TPE as the predominant species. For the ¹H NMR spectrum of TPE see C.-H. Ying, S.-B. Yan, W.-L. Duan, *Organic Letters* **2014**, *16*.

4.0. NMR characterization of cyclobutene 6 and rubrene endoperoxide

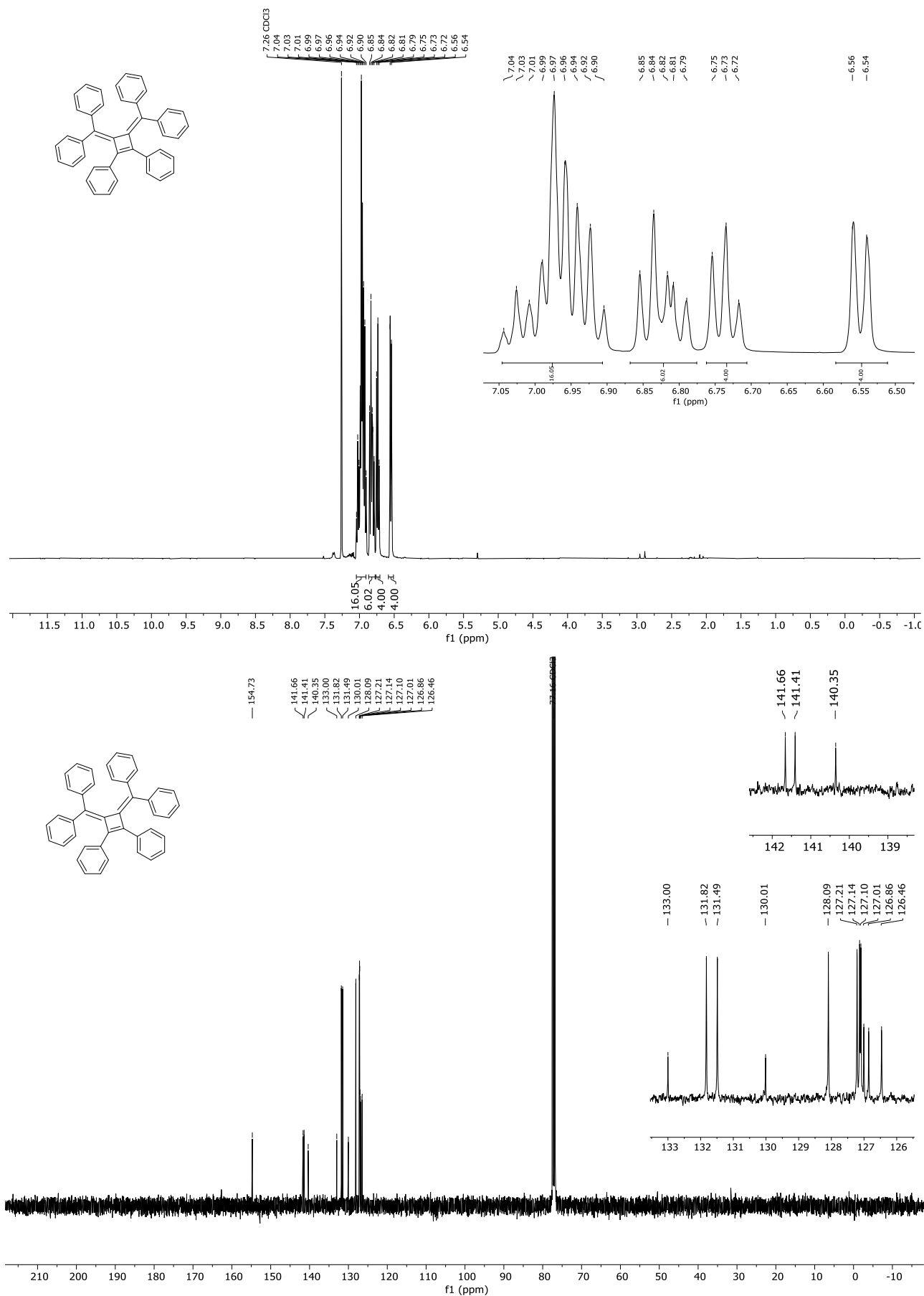
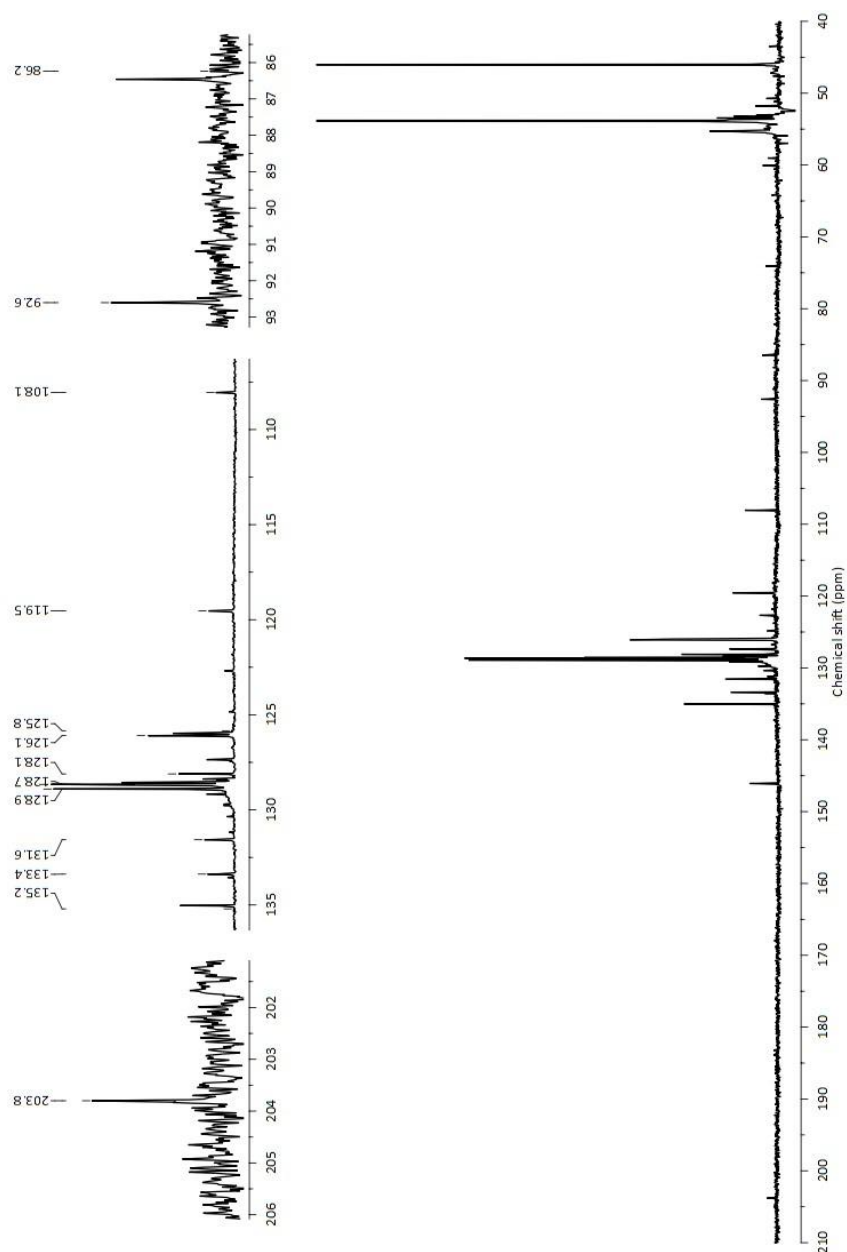
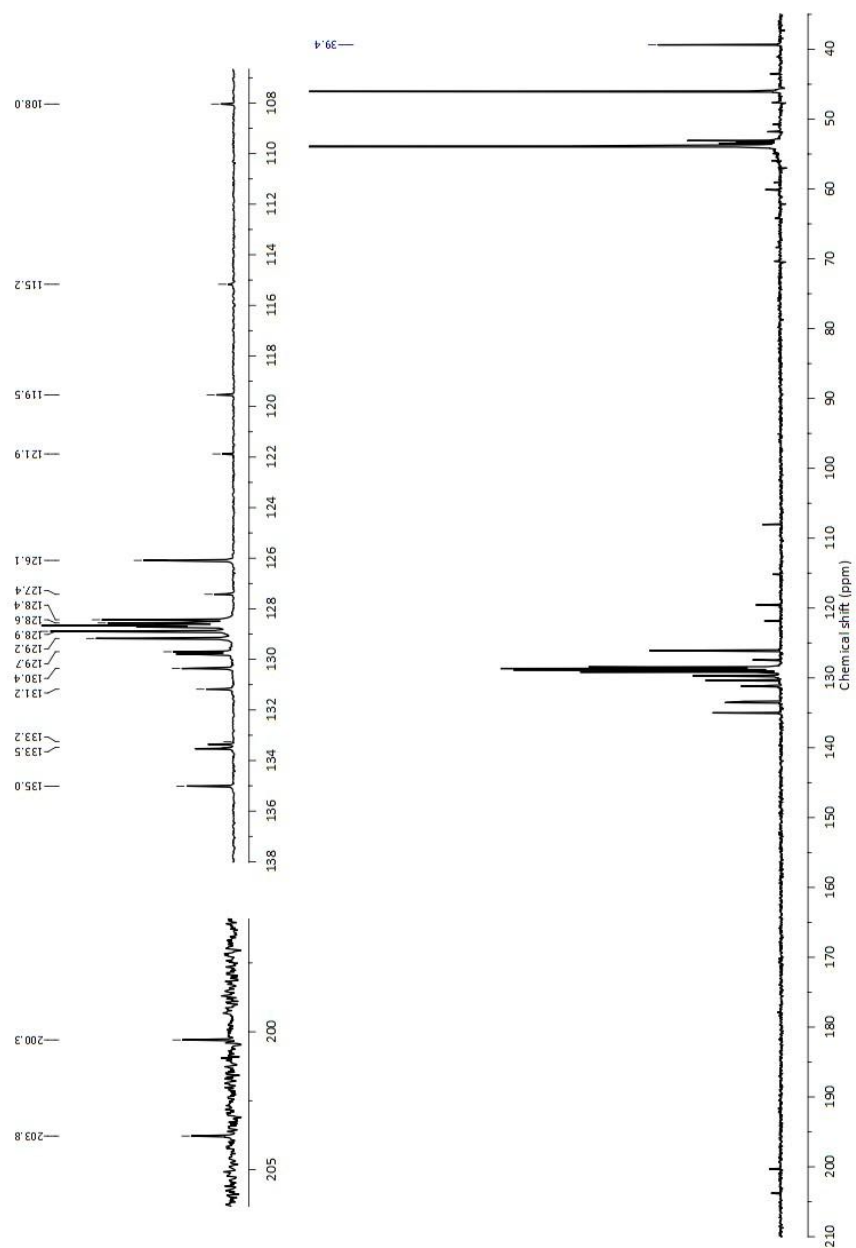


Figure S26. ^1H NMR (500 MHz, CDCl_3) and ^{13}C NMR (125 MHz, CDCl_3) spectra of the isolated cyclobutene 6.

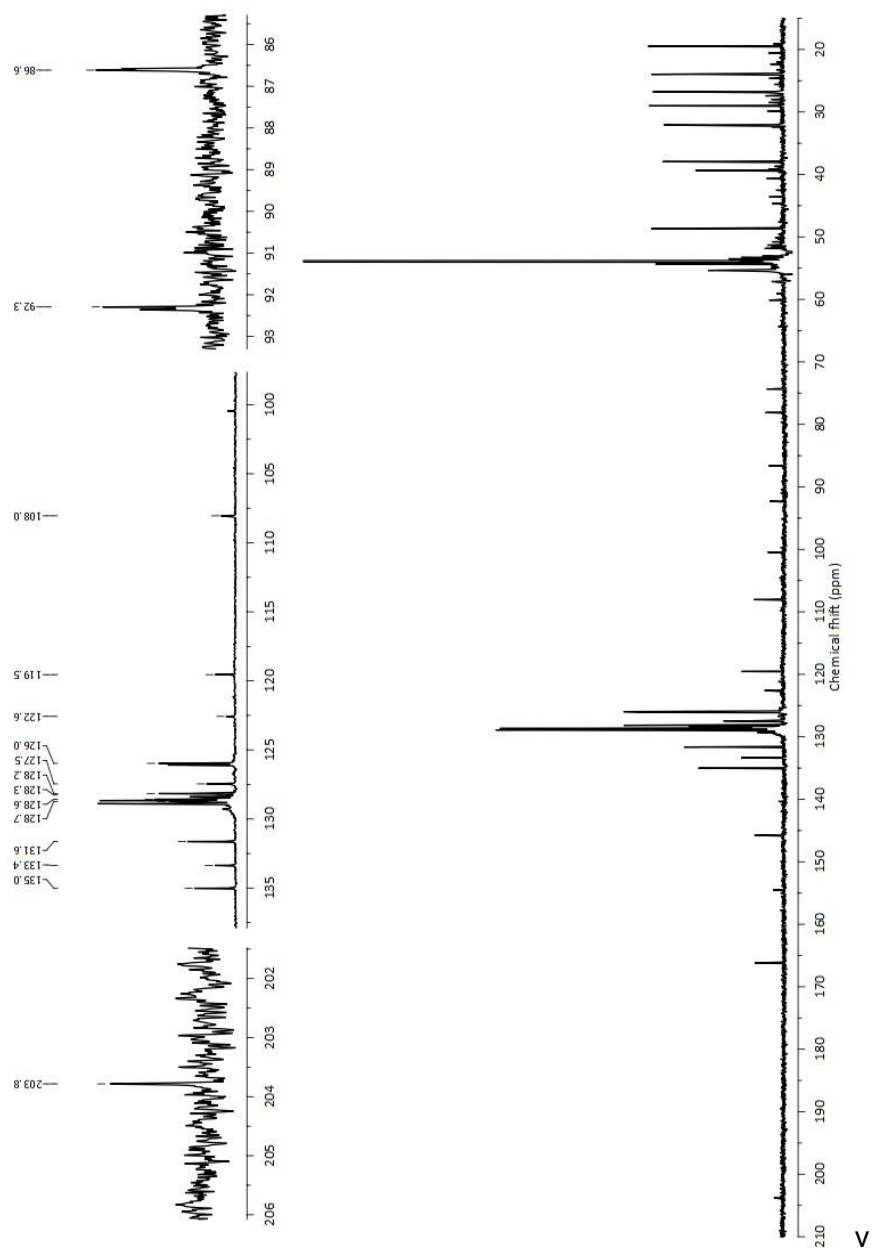
5.0. ^{13}C NMR UDEFT spectra



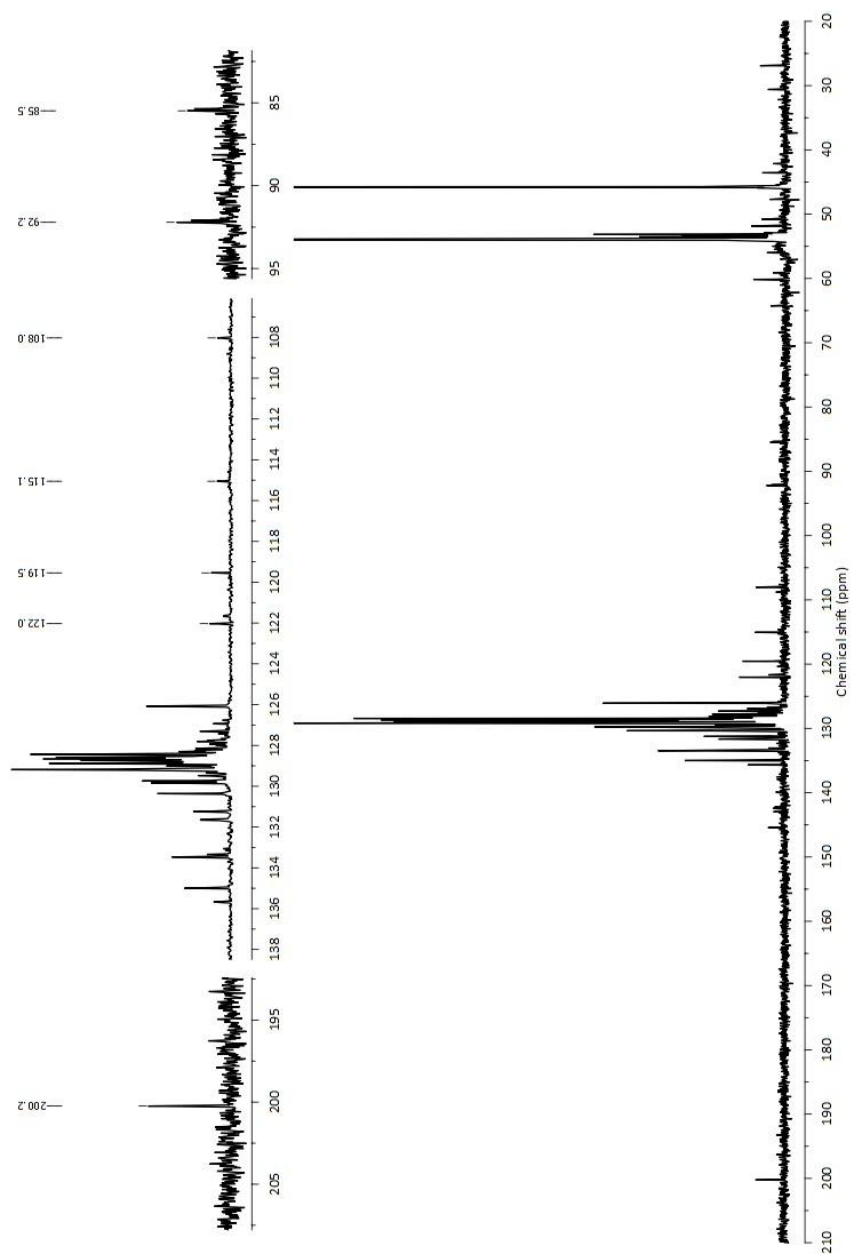
UDEFT_1 ^{13}C NMR UDEFT spectrum (125 MHz, CD_2Cl_2) of the reaction crude obtained by treating TPPA with oxalyl chloride and TEA.



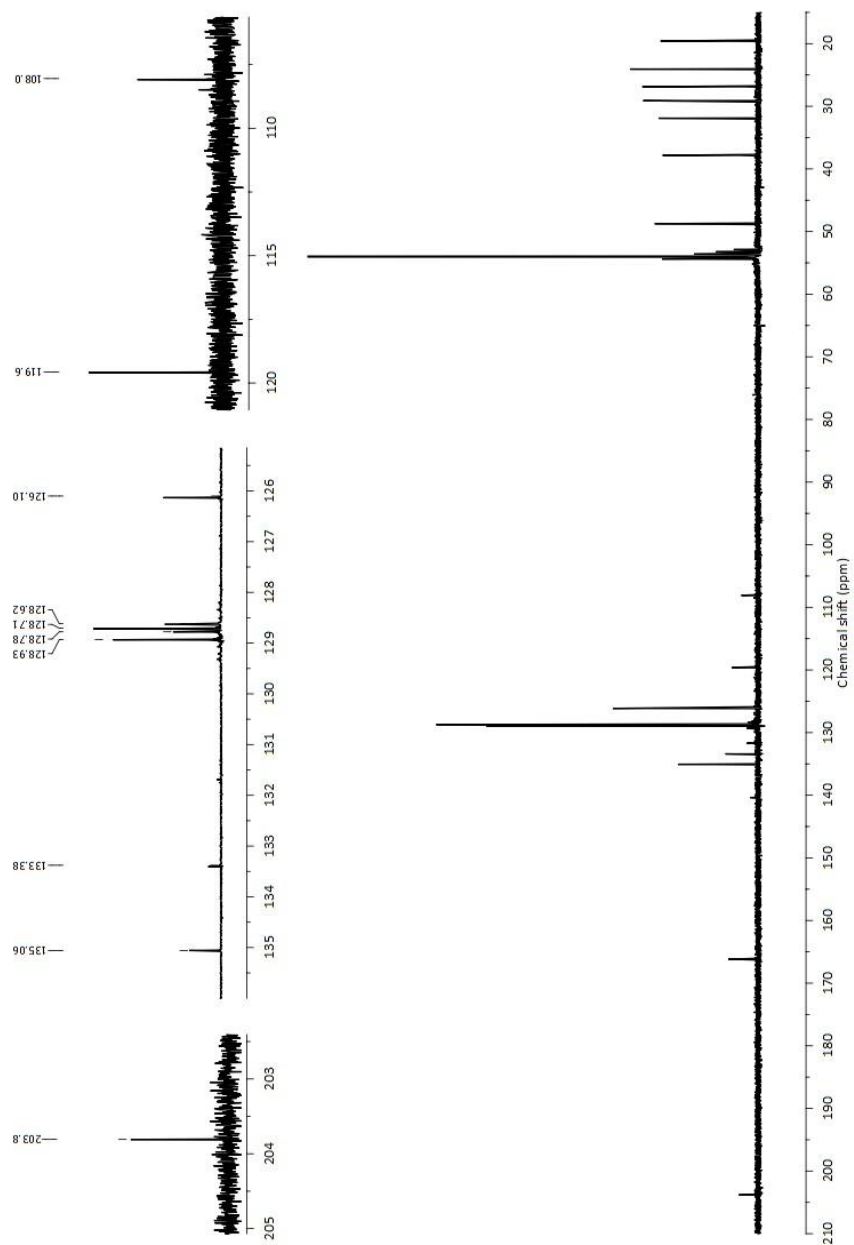
UDEFT_2 ^{13}C NMR UDEFT spectrum (125 MHz, CD_2Cl_2) of the reaction crude obtained by treating TPPA with MsCl and TEA.



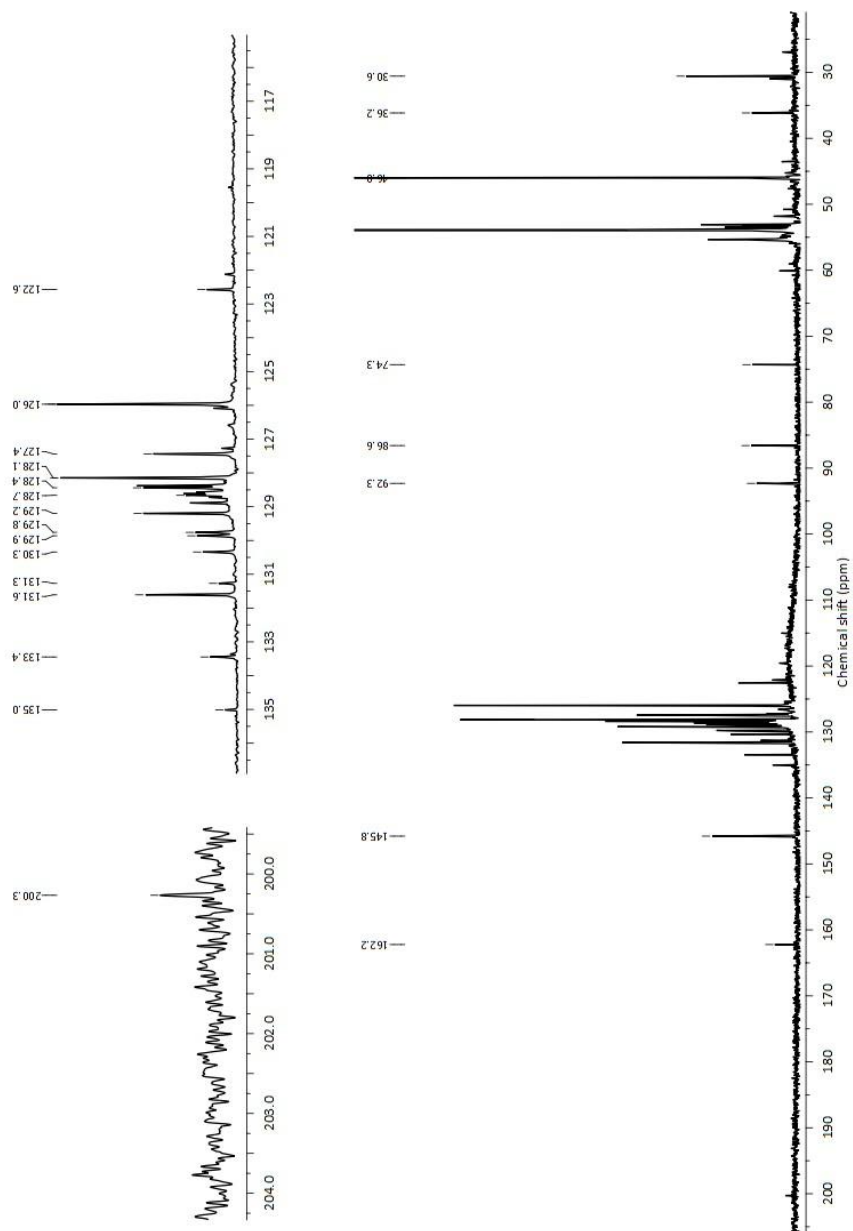
UDEFT_3 ^{13}C NMR UDEFT spectrum (125 MHz, CD_2Cl_2) of the reaction crude obtained by treating TPPA with MsCl and DBU.



UDEFT_4 ^{13}C NMR UDEFT spectrum (125 MHz, CD_2Cl_2) of the reaction crude obtained by treating TPPA with PCl_5 and TEA.



UDEFT_5 ^{13}C NMR UDEFT spectrum (125 MHz, CD_2Cl_2) of the reaction crude obtained by treating TPPA with PCl_5 and DBU.



UDEFT_6 ^{13}C NMR UDEFT spectrum (125 MHz, CD_2Cl_2) of the reaction crude obtained by treating TPPA with the Vilsmeier reagent and TEA.